Photoinduced Energy And Electron Transfer In Fullerene−oligothiophene−fullerene Triads

ARTICLE *in* THE JOURNAL OF PHYSICAL CHEMISTRY A · JUNE 2000

Impact Factor: 2.69 · DOI: 10.1021/jp0012597 · Source: OAI

6 AUTHORS, INCLUDING:

Stefan Meskers
Technische Universiteit Eindhoven
197 PUBLICATIONS **6,664** CITATIONS

Photoinduced Energy and Electron Transfer in Fullerene−Oligothiophene−Fullerene Triads

Paul A. van Hal,[†] Joop Knol,[‡] Bea M. W. Langeveld-Voss,[†] Stefan C. J. Meskers,[†] J. C. Hummelen,[‡] and René A. J. Janssen*,[†]

Laboratory of Macromolecular and Organic Chemistry, Eindhoven University of Technology, PO Box 513, 5600 MB Eindhoven, The Netherlands, and Stratingh Institute & Materials Science Center, University of Groningen, Nijenborgh 4, 9747 AG Groningen, The Netherlands

Received: March 31, 2000

A series of fullerene−oligothiophene−fullerene (C_{60}−*n*T−C_{60}) triads with $n = 3$, 6, or 9 thiophene units has been synthesized, and their photophysical properties have been studied using photoinduced absorption and fluorescence spectroscopy in solution and in the solid state as thin films. The results are compared to those of mixtures of oligothiophenes (*n*T) with *N*-methylfulleropyrrolidine (MP−C_{60}). Photoexcitation of the triads in the film results in an electron-transfer reaction for $n = 6$ and 9, but not for $n = 3$. The lifetime of the charge-separated state in the film is on the order of milliseconds. Photoexcitation of the oligothiophene moiety of the C_{60}−*n*T−C_{60} triads, dissolved in an apolar solvent, results in a singlet energy-transfer reaction to the fullerene moiety with rates varying between 10^{12} and 10^{13} s^{-1}. In more polar solvents, an *intra*molecular photoinduced charge separation occurs for $n = 6$ and 9 and, to some extent, for $n = 3$. The quenching of the MP−C_{60}(S_1) fluorescence provides a lower limit to the rate of the *intra*molecular photoinduced electron transfer of 10^{11} s^{-1} in the C_{60}−*n*T−C_{60} triads with $n = 6$ or 9 in polar solvents, assuming that charge separation occurs after singlet energy transfer from *n*T(S_1) to MP−C_{60}(S_1). A direct mechanism, i.e., charge separation from *n*T(S_1), cannot be excluded experimentally but must occur in the femtosecond time domain to compete effectively with energy transfer. The lifetime of the *intra*molecularly charge-separated state in the C_{60}−*n*T−C_{60} triads is significantly reduced compared to the lifetime of the radical ions in the films, and hence, the latter results from charge migration to different molecular sites. Similar energy- and electron-transfer reactions occur *inter*molecularly in solution from the *n*T and MP−C_{60} triplet states. The preferences for *intra*- and *inter*molecular energy- and electron-transfer reactions, as a function of conjugation length and solvent permittivity, are in full agreement with predictions that can be made using the Weller equation for the change in free energy upon charge separation.

Introduction

In recent years, composite films consisting of conjugated polymers and fullerene derivatives have been considered for achieving solid-state polymer photovoltaic cells.[1,2] The underlying photophysical process is an electron-transfer reaction from the conjugated polymer as a donor to the fullerene as an electron acceptor upon photoexcitation. One of the most remarkable features of conjugated polymer/fullerene blends is the fact that an ultrafast forward electron-transfer reaction occurs (<1 ps)[3] but the recombination of photogenerated electrons on the fullerene and holes on the polymer is slow and extends into the millisecond time domain.[4] As a result of the fast forward electron transfer, the quantum yield for the photoinduced charge separation in these composite films is near unity. Therefore, the efficiency of photovoltaic devices is probably limited by the transport or the injection of charges to the electrodes. Apart from the low charge-carrier mobility generally associated with conjugated polymers and fullerenes, an important reason for inefficient charge transport is the random nature of the interpenetrating network, which is formed spontaneously by spin coating mixtures of *p*-type π-conjugated polymer and fullerene derivatives.[5]

In addition to conjugated polymer/fullerene blends, various molecular dyads and triads of fullerenes involving covalent bonds to organic donors such as aromatic amines;[6] oligothiophenes;[7] oligo(*p*-phenylenevinylene)s;[8] oligo(thienylenevinylene)s;[9] tetrathiafulvalenes;[10] carotenes;[11] porphyrins;[12] phthalocyanines;[13] phytochlorins;[14] or organometallic donors with ruthenium,[15] ferrocene,[16] and copper[17] have been described in recent years. The preparation and photophysical properties of these molecular arrays involving fullerenes have recently been reviewed.[18] A general feature of these molecular donor−acceptor systems is that the lifetime of the charge-separated state does not extend into the millisecond regime as for the polymer/fullerene composites, but is limited to the low nanosecond time domain, although some exceptions to this general rule exist.[6e,10b,12e,m,16a]

To investigate whether the large difference in forward and backward electron-transfer rates in polymer/fullerene composites is an intrinsic property of the molecules involved or a material property, we set out to explore the photoinduced electron transfer in molecular triads of conjugated oligothiophenes covalently linked to fullerenes, i.e., C_{60}−*n*T−C_{60} ($n = 3$, 6, and 9) (Figure 1). These well-defined acceptor−donor−acceptor triad molecules can be studied as isolated molecules in solution and in the solid state where *inter*molecular interactions occur. By using different solvents, it is possible to address the effect of the polarity of the medium on the photoinduced charge separation

* Author to whom correspondence should be addressed. E-mail: R.A.J.Janssen@tue.nl.
[†] Eindhoven University of Technology.
[‡] University of Groningen.

10.1021/jp0012597 CCC: $19.00
Published on Web 06/03/2000

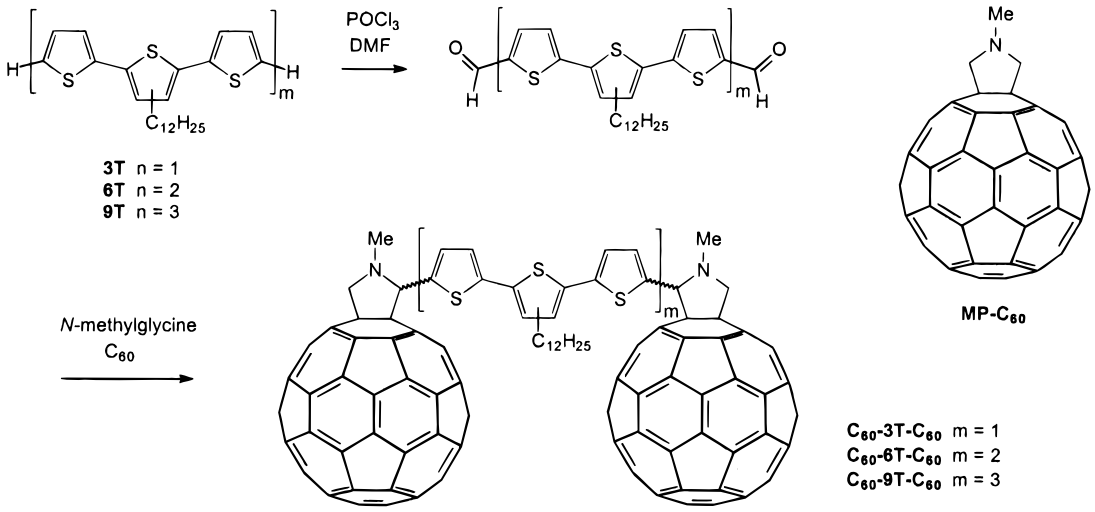

Figure 1. Synthesis of the $C_{60}-n$T$-C_{60}$ fullerene−oligothiophene−fullerene triads.

and recombination. The covalent linkage of the oligothiophene and fullerene also enforces a spatial ordering of the donor and acceptors in the solid state, which is not achieved in the blend. This spatial restriction may be considered as a first step in preparing predefined architectures of structurally organized donor and acceptor phases on a nanoscopic scale. We expect that such nanoscopic structures may hold the key to more efficient polymer photovoltaic cells.

Here, we describe the synthesis of these novel triads and investigate their photophysical properties in solid films and in solutions of different polarity using (time-resolved) fluorescence and photoinduced absorption (PIA) spectroscopy. The results are compared to those for simple mixtures of the *n*T oligothiophenes with *N*-methylfulleropyrrolidine (MP−C_{60}). We demonstrate that both energy- and electron-transfer reactions occur upon photoexcitation of the $C_{60}-n$T$-C_{60}$ triads on short time scales. The energy and electron transfer can take place from the singlet as well as from the triplet excited states of both the oligothiophene and the fullerene. The discrimination between the energy- and electron-transfer processes strongly depends on the permittivity of the medium, and we show that the transfer can be qualitatively modeled with the Weller equation. We show that the long lifetime in the solid state results from the migration of opposite charges to different sites and is not associated with an *intra*molecular charge-separated state.

Results and Discussion

Synthesis. The oligothiophenes used as starting materials (Figure 1) in the synthesis of the $C_{60}-n$T$-C_{60}$ triads carry a dodecyl substituent on one of the β positions of every third thiophene ring, starting at the second ring.[19,20] As a consequence, the 6T and 9T triads are mixtures of three and four regioisomers, respectively. The oligothiophenes were converted to the corresponding α,ω-dialdehydes in a Vilsmeier−Haack reaction with phosphorus oxychloride and *N*,*N*-dimethylformamide. The triads ($C_{60}-n$T$-C_{60}$; $n = 3$, 6, and 9) were prepared in a 1,3 dipolar cycloaddition reaction by treating the dialdehydes with 8 equiv of *N*-methylglycine and 4 equiv of [60]fullerene (C_{60}) in chlorobenzene at reflux temperature for 18 h. This reaction creates a stereocenter at each pyrrolidine ring. Hence, the three triads are obtained as mixtures of stereoisomers. In combination with the regioisomerism of the oligothiophenes, 4 $C_{60}-3$T$-C_{60}$ isomers, 10 $C_{60}-6$T$-C_{60}$ isomers, and 16 $C_{60}-9$T$-C_{60}$ isomers are expected. The structure and purity of the $C_{60}-n$T$-C_{60}$ triads was confirmed with ^{1}H NMR, ^{13}C NMR, UV−Vis spectroscopy, MALDI-TOF-MS, and HPLC. Both NMR and HPLC analyses of the triads clearly showed the presence of several stereoisomers. *N*-methylfulleropyrrolidine (MP−C_{60}) was used as a reference compound and was synthesized according to published methods.[6j]

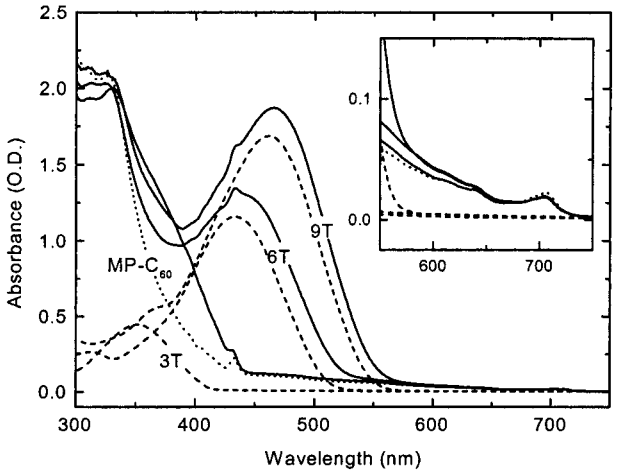

Figure 2. UV−Vis absorption spectra of MP−C_{60} (4.6×10^{-4} M, dotted line), $C_{60}-n$T$-C_{60}$ (2.3×10^{-4} M, solid lines), and *n*T (2.3×10^{-4} M, dashed lines) for $n = 3$, 6, and 9 recorded in *o*-dichlorobenzene at 295 K with a 1-mm path length. The inset shows an enlarged view of the 550−750 nm region.

Absorption Spectra of $C_{60}-n$T$-C_{60}$. The absorption spectra of the $C_{60}-n$T$-C_{60}$ triads closely correspond to a superposition of the individual spectra of *n*T and MP−C_{60} (Figure 2). Hence, electron transfer between donor and acceptor does not occur in the ground state. As expected, a significant red shift of the absorption maximum and an increase in the molar absorption coefficient occurs with increasing conjugation length. The inset of Figure 2 shows that, at 600 nm, the absorption of the *n*T oligomers is negligible, and hence, this wavelength can be used to selectively excite the fullerene moiety. For $C_{60}-6$T$-C_{60}$ and $C_{60}-9$T$-C_{60}$, light of 430−470 nm will result in almost selective excitation of the oligothiophene moiety, but selective excitation of the terthiophene unit in $C_{60}-3$T$-C_{60}$ is not possible.

Photoexcitation of $C_{60}-n$T$-C_{60}$ as Thin Films at 80 K. Thin films of $C_{60}-n$T$-C_{60}$ were obtained by casting from solution on quartz substrates. The films were studied by PIA in the microsecond and millisecond time domains using a mechanically modulated laser excitation beam and phase-sensitive

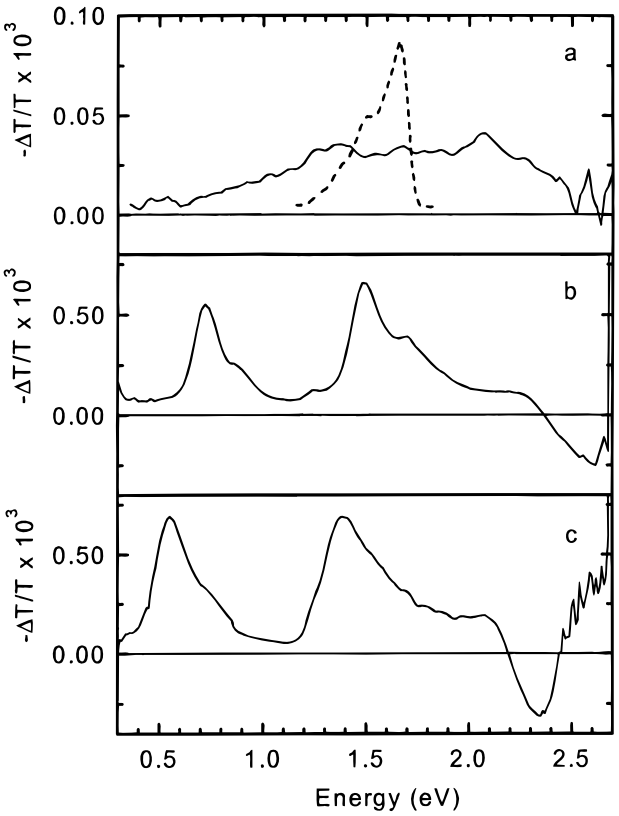

Figure 3. PIA spectra (solid lines) of $C_{60}-n$T$-C_{60}$ thin films on quartz for (a) $n = 3$, (b) $n = 6$, and (c) $n = 9$. The spectra were recorded at 80 K by excitation at 351.1 and 363.8 nm for $n = 3$ and at 457.9 nm for $n = 6$ and 9 with 25 mW and a modulation frequency of 275 Hz. In graph (a), the vertical scale has been expanded by 1 order of magnitude relative to those in (b) and (c). The PL spectrum of $C_{60}-3T-C_{60}$ is shown in (a) with a dashed line.

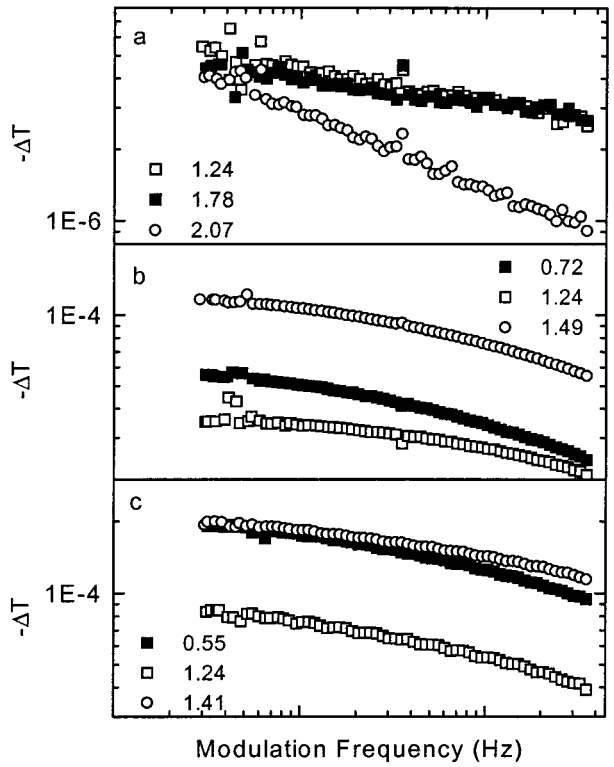

Figure 4. Modulation-frequency dependence of the PIA spectra shown in Figure 3 (peak positions are shown in the insets) for (a) $n = 3$, (b) $n = 6$, and (c) $n = 9$. The frequency dependencies were recorded at 80 K by excitation at 351.1 and 363.8 nm for $n = 3$ and at 457.9 nm for $n = 6$ and 9 with 25 mW.

lock-in detection over a wide energy range from 0.25 to 3.5 eV, i.e., covering the UV/vis/IR spectral region. This technique is very sensitive for probing a small concentration of long-lived photoexcitations (detection limit $\Delta T/T \sim 10^{-6}$). The PIA spectra of thin films of $C_{60}-n$T$-C_{60}$ recorded at 80 K reveal that there is a strong difference in the excited states created for $C_{60}-3T-C_{60}$ in comparison with those for $C_{60}-6T-C_{60}$ and $C_{60}-9T-C_{60}$ (Figure 3). For $C_{60}-3T-C_{60}$, we observe a low intensity PIA spectrum that extends over the 1−2 eV region, whereas the spectra of $C_{60}-6T-C_{60}$ and $C_{60}-9T-C_{60}$ are much more intense and show two characteristic peaks in the visible and near-IR energy regions.

The exact assignment of the PIA spectrum of $C_{60}-3T-C_{60}$ is presently not known, but characteristic strong signals of the $3T^{+\bullet}$ radical cations (expected at about 1.46 and 2.25 eV[21]) are not observed. By varying the modulation frequency of the excitation beam (Figure 4a, Table 1), we found that the peak at 2.07 eV is probably of a different origin than the bands at 1.24 and 1.78 eV, although all bands increase similarly with pump intensity according to a power law ($-\Delta T \propto I^p$, with $p = 0.75-0.80$). These exponents indicate that the photoexcitations in $C_{60}-3T-C_{60}$ decay in a nearly monomolecular fashion, for which $p = 1$ is expected. We tentatively attribute the spectrum (at least in part) to a triplet state of the fullerene moiety. In addition to this triplet state, we observe a weak fluorescence for $C_{60}-3T-C_{60}$ with an onset at 1.66 eV due to emission from a fullerene singlet excited state (Figure 3a). The absence of $3T^{+\bullet}$ radical cations, the triplet-state fullerene PIA, and the fluorescence all indicate that photoinduced electron transfer is not an important process in thin films of $C_{60}-3T-C_{60}$.

TABLE 1: Energies of Optical Transitions of PIA Spectra of Thin Films of $C_{60}-n$T$-C_{60}$ Triads. Modulation Frequency (n) and Excitation Intensity Dependence (p) of PIA Signals

triad	PIA (eV)	n (ω^{-n})	p (I^p)
$C_{60}-3T-C_{60}$	1.24	0.14	0.76
	1.78	0.10	0.81
	2.07	0.33	0.75
$C_{60}-6T-C_{60}$	0.75	0.17	0.46
	1.24	0.12	0.48
	1.49	0.14	0.48
$C_{60}-9T-C_{60}$	0.54	0.14	0.48
	1.24	0.14	0.49
	1.41	0.11	0.47

In contrast, for a thin film of $C_{60}-6T-C_{60}$, the characteristic absorption bands of the $6T^{+\bullet}$ radical cation at 0.75 and 1.49 eV and of the MP$-C_{60}^{-\bullet}$ radical anion at 1.24 eV are present in the PIA spectrum (Figure 3b). The simultaneous observation of $6T^{+\bullet}$ and MP$-C_{60}^{-\bullet}$ radical ions gives direct spectral evidence of a photoinduced electron-transfer reaction. Under these conditions, no fluorescence of $C_{60}-6T-C_{60}$ is detected. The relative intensities of the PIA bands of $6T^{+\bullet}$ at 1.49 eV and of MP$-C_{60}^{-\bullet}$ at 1.24 eV are qualitatively consistent with the difference in molar absorption coefficients of these ions as determined in solution; for $6T^{+\bullet}$, $\epsilon = 72000$ M^{-1} cm^{-1}, and for $C_{60}^{-\bullet}$, $\epsilon = 12000$ M^{-1} cm^{-1}.[19,22] The PIA bands increase with the square root of the excitation intensity ($-\Delta T \propto I^p$, with $p = 0.46-0.48$; Table 1), which indicates a bimolecular decay process, consistent with the recombination of positive and negative charges. The decrease of $-\Delta T$ with increasing modulation frequency follows approximately the same power-law behavior for all bands ($-\Delta T \propto \omega^{-n}$, with $n = 0.12-0.17$; Figure 4b, Table 1) with increasing frequency ω between 30 and 4000 Hz. Such power-law behavior is characteristic for a distribution of lifetimes in the millisecond time domain. The fact that

changes in $-\Delta T$ with pump intensity and with modulation frequency are similar for the PIA bands attributed to $6T^{+\bullet}$ and $MP-C_{60}^{-\bullet}$ strongly suggests that these photogenerated radical ions decay via the same relaxation process. The PIA results for thin films of $C_{60}-9T-C_{60}$ are analogous to those of $C_{60}-6T-C_{60}$ (Figure 3c) and support a photoinduced electron-transfer reaction. The principal absorption bands of the $9T^{+\bullet}$ radical cations are observed at 0.55 and 1.41 eV, while a shoulder at 1.24 eV is consistent with the presence of $MP-C_{60}^{-\bullet}$ radical anions. The PIA bands decrease in similar fashion with increasing modulation frequency ($-\Delta T \propto \omega^{-n}$, with $n = 0.11-0.14$; Table 1, Figure 4c), and again, a square-root dependence for the pump intensity is observed ($-\Delta T \propto I^p$, with $p = 0.47-0.49$; Table 1). Fluorescence of $C_{60}-9T-C_{60}$ is absent.

The observation of a long-lived charge-separated state for the molecular triads $C_{60}-6T-C_{60}$ and $C_{60}-9T-C_{60}$ and the concurrent absence of charged states in $C_{60}-3T-C_{60}$ raises the question of whether these differences are consistent with energetic predictions based on relative oxidation and reduction potentials, excitation energies, and Coulombic stabilization. Furthermore, it is of interest to know whether the photoinduced electron-transfer reaction is an *intra*molecular or an *inter*molecular process. Previous studies on dyads and triads involving fullerenes have shown that the charge-separated state typically has a lifetime on the (sub)nanosecond time scale,[6−18] although some extend into the microsecond domain.[6e,10b,12e,m,16a]

We propose that a charge-separated state with a lifetime on the order of milliseconds, as observed for thin films of $C_{60}-6T-C_{60}$ and $C_{60}-9T-C_{60}$, results from migration of the hole and/or the electron to different molecules after the photoinduced electron-transfer reaction.[23] This proposition is corroborated by the nonlinear excitation intensity dependence of the PIA bands, which is a clear indication of bimolecular processes that require diffusion of photoexcited species. To obtain support for this proposition and to study the energetics of photoinduced electron-transfer reactions in these molecules in more detail, we have investigated the photoexcitation of $C_{60}-n$T$-C_{60}$ and mixtures of nT with $MP-C_{60}$ in solvents of different polarity.

Photoexcitation of *n*T and MP−C$_{60}$ in Solution. Before describing the photoexcitations of the $C_{60}-n$T$-C_{60}$ triads and mixtures of nT with $MP-C_{60}$, it is important to consider some of the photophysical properties of the individual components. Photoexcitation of the nT oligothiophenes in solution results in a transient singlet excited state nT(S_1), which decays by fluorescence to the ground state and by intersystem crossing to the nT(T_1) triplet state.[24,25] In solution, the quantum yields for fluorescence are high,[25] and intense fluorescence spectra of 3T, 6T, and 9T are observed in solution. The positions of the emission bands depend only slightly on the nature of the solvent (Table 2). The singlet excited-state lifetime τ of the nT oligomers has been determined in toluene solution from time-resolved fluorescence. τ decreases with conjugation length from 0.81 ns for 3T, to 0.78 ns for 6T, to 0.65 ns for 9T (Table 2). The value for 6T is close to the value of 1.10 ns reported for a related 6T derivative.[26] The triplet-state absorption spectra of 3T, 6T, and 9T have been recorded using PIA spectroscopy (Figure 5) in three solvents of increasing polarity: toluene, *o*-dichlorobenzene, and benzonitrile at a concentration of 2.3×10^{-4} M. The spectra invariably exhibit a $T_n \leftarrow T_1$ transition, which shifts to lower energy with increasing chain length. Again, the peak position is only slightly dependent on the nature of the solvent (Table 2). The intensity of the $T_n \leftarrow T_1$ absorptions increases linearly with pump intensity. The linear intensity dependence shows that triplet−triplet annihilation is not a major decay pathway under these conditions. A linear intensity dependence is expected for a monomolecular decay mechanism, but it should be noted that bimolecular mechanisms such as quenching of the nT(T_1) state by molecular oxygen would also give the same behavior. The lifetime of the photoexcitations has been determined by recording the change in transmission ($-\Delta T$) as a function of the modulation frequency (ω) in the range of 30−4000 Hz (Figure 6) and fitting the experimental data, after correction for the fluorescence contribution, to the analytical expression for monomolecular decay.[27]

$$-\Delta T \propto \frac{Ig\tau}{\sqrt{1+\omega^2\tau^2}} \qquad (1)$$

where g is the efficiency of generation of the photoinduced species and $1/\tau$ is the monomolecular decay constant. The lifetime of the nT(T_1) triplet state decreases with chain length from ~400 μs for 3T to ~100 μs for 9T (Table 2). The triplet state energies of α-oligothiophenes have recently been determined independently by photodetachment photoelectron spectroscopy (nT, with $n = 1-4$) and spectroscopic and calorimetric measurements (nT, with $n = 1-5$ and 7).[28] For 3T, the triplet energy is 1.92−1.93 eV. From the linear relation of the triplet energy as a function of the reciprocal n,[28b] it is possible to estimate the triplet energy levels for 6T (~1.64 eV) and 9T (~1.55 eV).

In addition to the triplet-state transitions, small signals of photochemically generated nT$^{+\bullet}$ radical cations are observed in the PIA spectra of the nT oligomers dissolved in *o*-dichlorobenzene and benzonitrile. The direct photogeneration

TABLE 2: Spectroscopic Data for *n*T Oligomers and MP−C$_{60}$ in Different Solvents

	solvent	$S_1 \leftarrow S_0$ (eV)	$S_1 \rightarrow S_0$ (eV)	$\tau(S_1)$ (ns)	$T_n \leftarrow T_1$ (eV)	$\tau(T_1)$ (μs)
3T	$PhCH_3$	3.56	3.00	0.81	2.63	410
	ODCB	3.52	2.97		2.59	310
	PhCN	3.50	2.98		2.62	380
6T	$PhCH_3$	2.92	2.42	0.78	1.78	145
	ODCB	2.86	2.39		1.76	140
	PhCN	2.86	2.39		1.79	154
9T	$PhCH_3$	2.74	2.26	0.65	1.59	93
	ODCB	2.68	2.22		1.55	127
	PhCN	2.69	2.24		1.56	
$MP-C_{60}$	$PhCH_3$	1.76	1.74	1.45	1.78	240
	ODCB	1.76	1.73		1.78	190
	PhCN	1.75	1.73		1.79	220

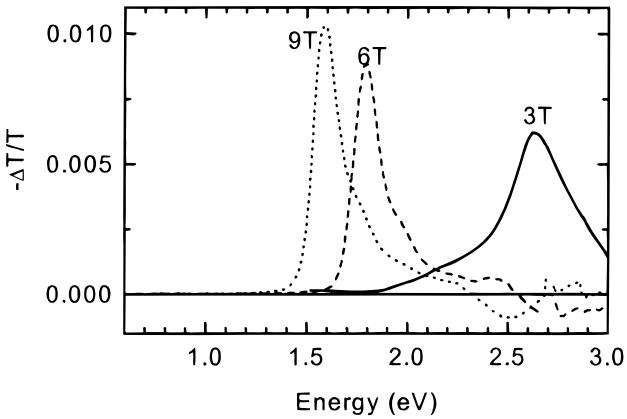

Figure 5. PIA spectra of oligothiophenes nT (n = 3, 6, and 9) in toluene solution (2.3×10^{-4} M) at 295 K. Recorded with 50-mW excitation at 351.1 and 363.8 nm for 3T and at 457.9 nm for 6T and 9T.

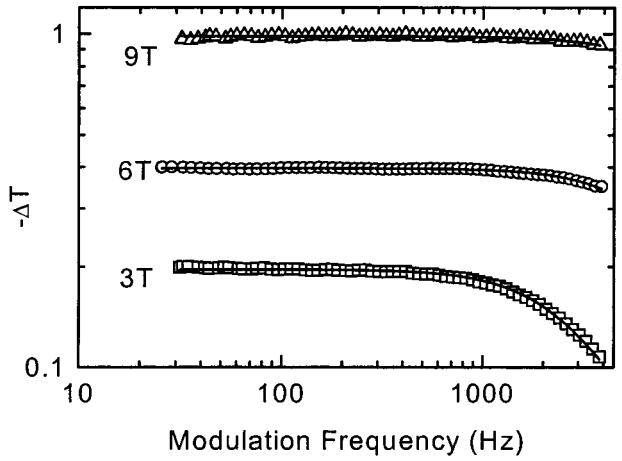

Figure 6. Modulation-frequency dependence of the PIA spectra of *n*T dissolved in toluene (Figure 5). The frequency dependencies were recorded with 50 mW excitation at 351.1 and 363.8 nm for 3T and at 457.9 nm for 6T and 9T. Solid lines represent least-squares fits to the expression for monomolecular decay with lifetimes of 410 μs for 3T, 145 μs for 6T, and 93 μs for 9T.

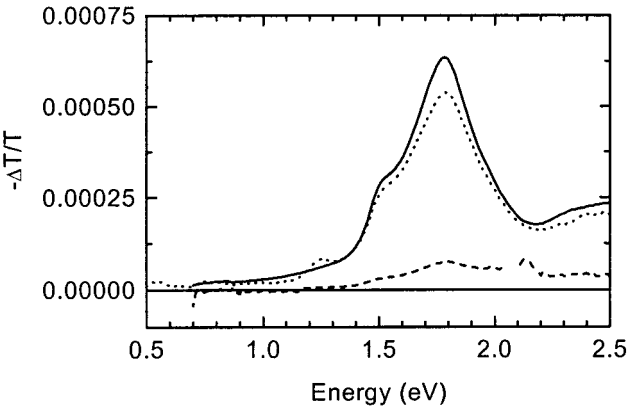

Figure 7. PIA spectra of MP−C_{60} in *o*-dichlorobenzene (4.6×10^{-4} M) at 295 K, recorded with excitation at 457.9 nm (solid line) and 600.0 nm (dashed line). The PIA spectrum of MP−C_{60} in benzonitrile solution (4.6×10^{-4} M, 457.9 nm) is shown with a dotted line.

of charged excitations of oligothiophenes is known to involve an electron-transfer reaction from the singlet excited *n*T(S_1) state to the solvent.[21,29,30] The formation of radical cations depends on the solvent used, but solvent polarity is not the pertinent criterion. In general, the back electron transfer between radical cation and solvent radical anion is expected to be fast, unless the solvent exhibits an irreversible dissociative electron-capture reaction, which is a well-known process for chlorinated solvents ($RCl + e^- \rightarrow R^\bullet + Cl^-$). As a result, the charged excitations produced in this way have long lifetimes on the order of $\tau =$ 20 ms.

Photoexcitation of MP−C_{60} in toluene, *o*-dichlorobenzene, or benzonitrile (4.6×10^{-4} M) results in a weak fluorescence at 1.74 eV and a long-lived triplet state. The fluorescence quantum yield of MP−C_{60} is known to be only 6×10^{-4}, and the triplet state is formed with a quantum yield near unity.[6i] The lifetime of the MP−C_{60}(S_1) state determined from time-resolved fluorescence is 1.45 ns (Table 2), close to the value of 1.28 ns previously reported.[6i] The PIA spectrum of the MP−C_{60}(T_1) state exhibits a peak at 1.78 eV with a characteristic shoulder at 1.54 eV (Figure 7). The molar absorption coefficient of this $T_n \leftarrow T_1$ absorption is 16000 M cm^{-1}.[6i] Similar PIA spectra have been obtained with excitation at 363.8, 457.9, or 600 nm. The lifetime of the MP−C_{60}(T_1) state in solution at

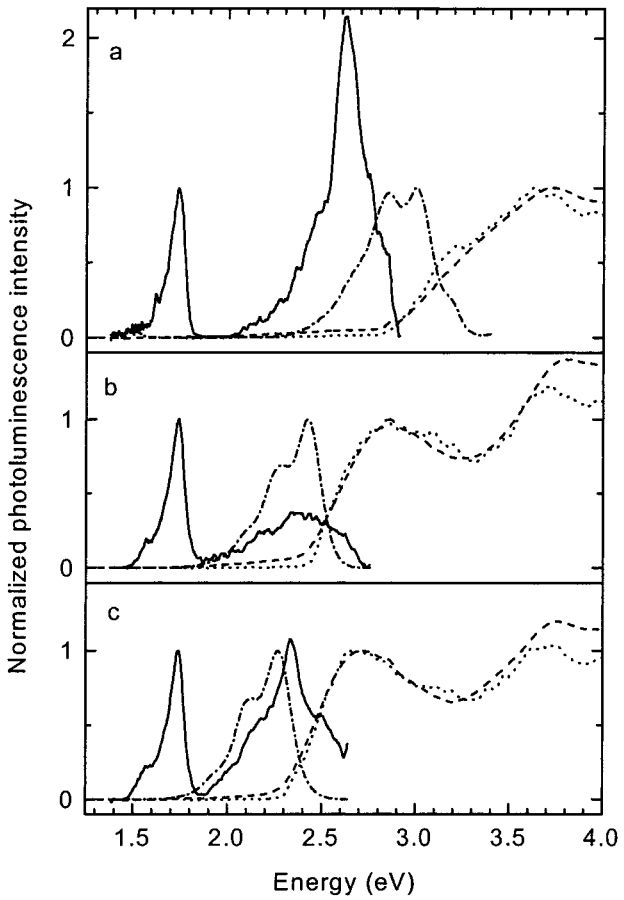

Figure 8. Normalized fluorescence (solid lines), absorption (dashed lines), and excitation (dotted lines) spectra of C_{60}−*n*T−C_{60} in toluene solution for (a) $n = 3$, (b) $n = 6$, and (c) $n = 9$. The spectra were recorded at 295 K by excitation at 350 nm for $n = 3$, at 433 nm for $n = 6$, and at 457 nm for $n = 9$. The emission spectra of the C_{60}−*n*T−C_{60} triads were corrected for Raman scattering of toluene, but residual Raman bands are clearly present at 2.62 eV for $n = 3$. The excitation spectra were recorded by monitoring the fullerene emission at 715 nm (1.73 eV). For a direct comparison, the normalized fluorescence spectra of the *n*T oligomers are included (dashed−dotted lines).

295 K is around 200 μs (Table 2). The triplet energy level of MP−C_{60} has been determined from phosphorescence to be 1.50 eV,[6b,6i,16a] slightly below the triplet energy of C_{60} at 1.57 eV.[31] The energy of the MP−C_{60}(T_1) state at 1.50 eV is less than the values reported and extrapolated for 3T, 6T, and 9T.[28] In benzonitrile, the PIA spectrum of MP−C_{60} reveals an extra small band of the radical anion of MP−C_{60} at 1.25 eV in addition to the signal of MP−C_{60}(T_1) (Figure 7). The formation of MP−$C_{60}^{-\bullet}$ is a result of the presence of a small amount of isocyanobenzene (PhNC) in benzonitrile (PhCN), which acts as a donor to MP−C_{60}(T_1). This is a bimolecular reaction, and the lifetime of the anions formed is long because charge recombination is hampered by follow-up reactions of the isocyanobenzene cation radical, which acts as a sacrificial electron donor.

Photoexcitation of C_{60}−*n*T−C_{60} and Mixtures of *n*T and MP−C_{60} in Toluene. In toluene solutions, the fluorescence of the oligothiophene moieties of the C_{60}−*n*T−C_{60} triads is strongly quenched with respect to the emission of the unsubstituted *n*T oligomers (Figure 8). Apart from some residual oligothiophene emission, the fluorescence spectra show a characteristic band at 1.73 eV, which results from emission from the MP−C_{60}(S_1) state. The excitation spectra of the fullerene emission coincide with the absorption spectra of the C_{60}−*n*T−

TABLE 3: Fluorescence Quenching of Triads [$\phi(n\mathrm{T})/\phi$ and $\phi(\mathrm{C_{60}})/\phi$] and Rate Constants for Energy Transfer (k_{ET}), Indirect Charge Separation (k_{CS}^{i}), and Direct Charge Separation (k_{CS}^{d})[a]

		$\phi(n\mathrm{T})/\phi$	k_{ET} (s^{-1})	$\phi(\mathrm{C_{60}})/\phi$	k_{CS}^{i} (s^{-1})	k_{CS}^{d} (s^{-1})
$PhCH_3$	$C_{60}-3T-C_{60}$	700	8.6×10^{11}	1		
	$C_{60}-6T-C_{60}$	9600	1.2×10^{13}	1		
	$C_{60}-9T-C_{60}$	5900	9.1×10^{12}	1		
ODCB	$C_{60}-3T-C_{60}$			2	6.9×10^{8}	8.6×10^{11}
	$C_{60}-6T-C_{60}$			75	5.1×10^{10}	9.1×10^{14}
	$C_{60}-9T-C_{60}$			150	1.2×10^{11}	1.4×10^{15}
PhCN	$C_{60}-3T-C_{60}$			5	2.8×10^{9}	3.5×10^{12}
	$C_{60}-6T-C_{60}$			150	1.2×10^{11}	1.8×10^{15}
	$C_{60}-9T-C_{60}$			150	1.2×10^{11}	1.4×10^{15}

[a] Rate constants for energy transfer (k_{ET}), indirect charge separation (k_{CS}^{i}), and direct charge separation (k_{CS}^{d}) calculated from eqs 2, 5, and 6, respectively.

C_{60} triads. In fact, the fullerene fluorescence quantum yield of the $C_{60}-n\mathrm{T}-C_{60}$ triads in toluene is nearly identical to that of $MP-C_{60}$, irrespective of the excitation wavelength. The emission spectra of the $C_{60}-n\mathrm{T}-C_{60}$ triads shown in Figure 8 were corrected for Raman scattering of toluene, but residual Raman bands are clearly present at 2.62 eV for $C_{60}-3T-C_{60}$ for which an excitation wavelength of 350 nm is used. Hence, an accurate determination of the extent of fluorescence quenching of the oligothiophene emission is somewhat hampered by these artifacts. Best estimates for the quenching factors [$\phi(n\mathrm{T})/\phi$] are 700 for $C_{60}-3T-C_{60}$, 9600 for $C_{60}-6T-C_{60}$, and 5900 for $C_{60}-9T-C_{60}$ (Table 3). The fluorescence quenching of the oligothiophenes and the simultaneous emission of the $MP-C_{60}$ moiety are clear characteristics of an efficient *intra*molecular energy-transfer reaction of the $n\mathrm{T}(S_1)$ state to the $MP-C_{60}(S_1)$ state. The quenching and the fluorescence lifetimes of the pristine *n*T oligomers (Table 2) can be used to estimate the rate constants for the energy-transfer reaction (k_{ET}) via the relation

$$k_{ET} = \left[\frac{\phi(n\mathrm{T})}{\phi} - 1\right]/\tau(n\mathrm{T}) \qquad (2)$$

Here, $\phi(n\mathrm{T})/\phi$ is the quenching ratio, and $\tau(n\mathrm{T})$ is the lifetime of the S_1 state (Table 2). The resulting values collected in Table 3 show that the energy-transfer process is extremely fast and occurs within about 1 ps for $C_{60}-3T-C_{60}$ and within about 100 fs for $C_{60}-6T-C_{60}$ and $C_{60}-9T-C_{60}$.

The energy-transfer reaction from the $n\mathrm{T}(S_1)$ states, which populates the $MP-C_{60}(S_1)$ state, also affects the PIA spectra of the $C_{60}-n\mathrm{T}-C_{60}$ triads in comparison with those of the parent *n*T oligomers. The PIA spectra of $C_{60}-3T-C_{60}$ and $C_{60}-6T-C_{60}$ are identical to that of the $MP-C_{60}(T_1)$ state (Figure 9a). For both triads, the lifetime of the $MP-C_{60}(T_1)$ state is about 250 μs. This result demonstrates that the *intra*molecular singlet energy transfer to the fullerene moiety, as inferred from fluorescence quenching, is followed by efficient intersystem crossing to the $MP-C_{60}(T_1)$ state. In contrast, the PIA spectrum of $C_{60}-9T-C_{60}$ is significantly different and actually corresponds to a superposition of the $T_n \leftarrow T_1$ spectra of $9T(T_1)$ and $MP-C_{60}(T_1)$ (Figure 9a). The concurrent absence of a signal at ~0.70 eV shows that the PIA band at ~1.60 eV is not associated with $9T^{+\bullet}$. We conclude that the triplet energy of 9T is very close to the triplet energy of $MP-C_{60}$ (1.50 eV). On the basis of the quenching of the 9T fluorescence in $C_{60}-9T-C_{60}$, we propose that the $9T(T_1)$ state in $C_{60}-9T-C_{60}$ is formed after initial photoexcitation of 9T via a singlet energy transfer to $MP-C_{60}$, subsequent intersystem crossing to the $MP-C_{60}(T_1)$ state, and finally, a triplet energy transfer to 9T. In accordance with this model, the same PIA spectrum has been recorded when the fullerene moiety of $C_{60}-9T-C_{60}$ is selectively excited at 600 nm in toluene solution.

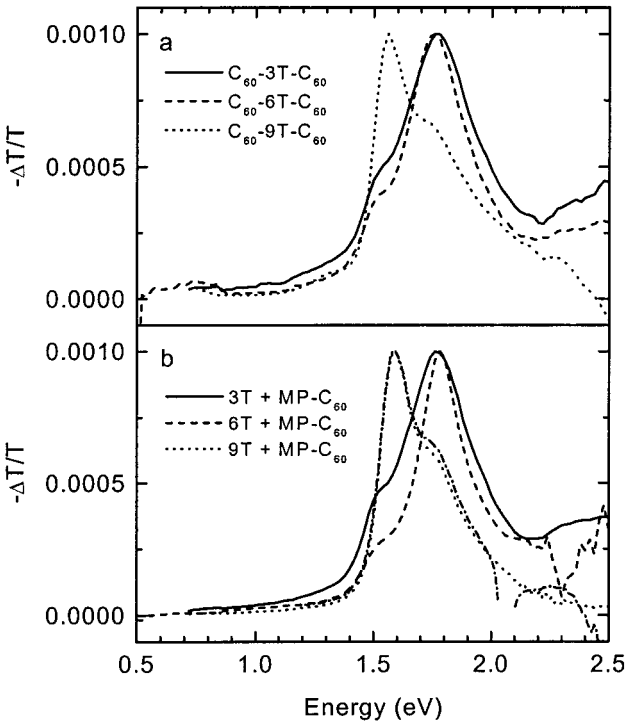

Figure 9. (a) PIA spectra of $C_{60}-n\mathrm{T}-C_{60}$ ($n = 3$, 6, and 9) in toluene (2.3×10^{-4} M) at 295 K recorded with excitation at 351.1 and 363.8 nm for $C_{60}-3T-C_{60}$ and at 457.9 nm for $C_{60}-6T-C_{60}$ and $C_{60}-9T-C_{60}$. (b) PIA spectra of mixtures of *n*T ($n = 3$, 6, and 9; 2.3×10^{-4} M) and $MP-C_{60}$ (4.6×10^{-4} M) in toluene at 295 K. The dashed−dotted line in graph (b) is for the $9T/MP-C_{60}$ mixture with excitation at 600 nm.

After photoexcitation of the *n*T oligomers in toluene solution containing $MP-C_{60}$ (a 1:2 molar proportion is used to mimic the ratio present in the triads), the $n\mathrm{T}(S_1)$ state decays via fluorescence and intersystem crossing. The PIA spectra of the mixtures of 3T or 6T with $MP-C_{60}$ give evidence for *inter*molecular triplet energy transfer from the $n\mathrm{T}(T_1)$ state to the lower lying $MP-C_{60}(T_1)$ state (Figure 9b), similar to previous observations for *n*T and C_{60}.[32] For 6T, the oligothiophene moiety can be nearly selectively excited at 458 nm, and the sole observation of the $MP-C_{60}(T_1)$ spectrum, and hence quenching of the $n\mathrm{T}(T_1)$ transitions, demonstrates the effectiveness of the *inter*molecular triplet energy-transfer reaction. As for $C_{60}-9T-C_{60}$, we observe only a partial quenching of the $9T(T_1)$ state by $MP-C_{60}$ (Figure 9b). Figure 9b shows that the same PIA spectra are obtained in mixtures of 9T and $MP-C_{60}$, regardless of whether 9T (at 458 nm) or $MP-C_{60}$ (at 600 nm) is selectively excited. Hence, in both cases, the same long-lived photoexcitations are eventually formed.

Photoexcitation of $C_{60}-n\mathrm{T}-C_{60}$ and Mixtures of *n*T and $MP-C_{60}$ in *o*-Dichlorobenzene and Benzonitrile. In more polar solvents such as *o*-dichlorobenzene and benzonitrile, a charge-separated state will be stabilized as a result of a screening of the Coulombic attraction of the opposite charges and solvation of the radical ions formed. Figure 10 shows the dramatic changes that occur in the fluorescence spectra of the three $C_{60}-n\mathrm{T}-C_{60}$ triads upon an increase in the polarity of the solvent from toluene ($\epsilon = 2.38$) to *o*-dichlorobenzene ($\epsilon = 9.93$) and to benzonitrile ($\epsilon = 25.20$). For $C_{60}-6T-C_{60}$ and $C_{60}-9T-C_{60}$, a near to complete quenching of the $MP-C_{60}(S_1)$ emission is observed in both *o*-dichlorobenzene and benzonitrile. For $C_{60}-3T-C_{60}$, a partial quenching of the $MP-C_{60}(S_1)$ state occurs,

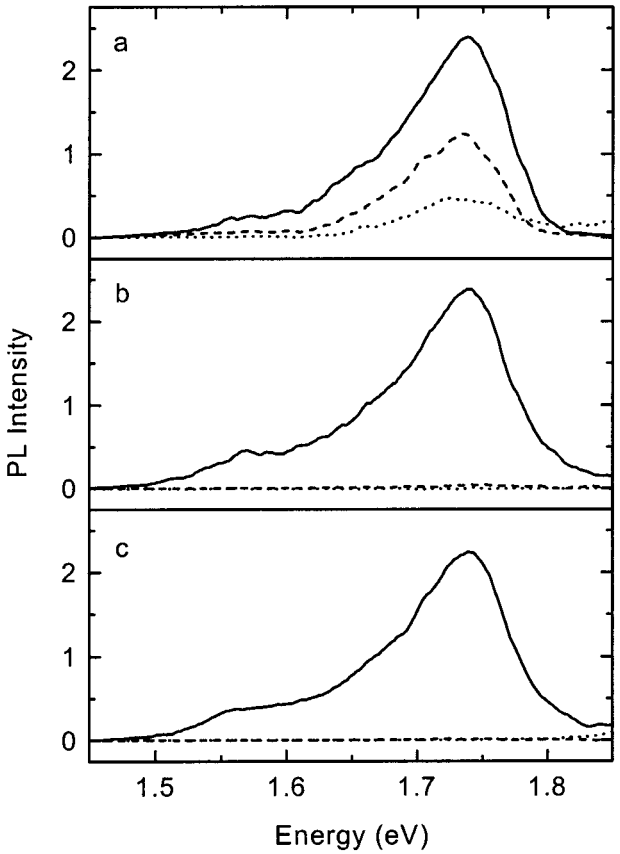

Figure 10. Fluorescence spectra of $C_{60}-n$T$-C_{60}$ in toluene (solid lines), *o*-dichlorobenzene (dashed lines), and benzonitrile (dotted lines) for (a) $n = 3$, (b) $n = 6$, and (c) $n = 9$. The spectra were recorded at 295 K by excitation at 350 nm for $n = 3$, at 433 nm for $n = 6$, and at 457 nm for $n = 9$. The optical density at the excitation wavelength was 0.1. The data have been corrected for differences in the index of refraction.

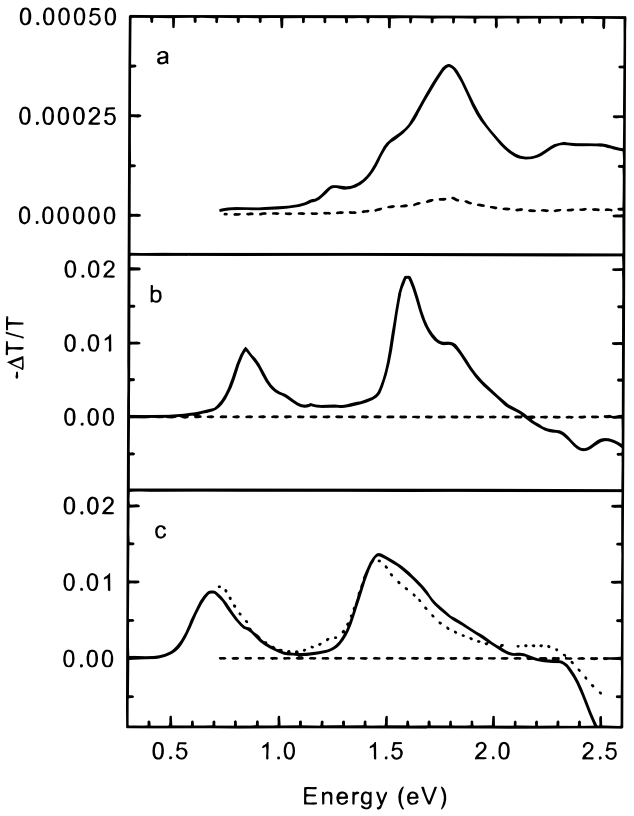

Figure 11. PIA spectra of *n*T (2.3×10^{-4} M) co-dissolved with MP$-C_{60}$ (4.6×10^{-4} M) (solid lines) and of corresponding $C_{60}-n$T$-C_{60}$ triads (2.3×10^{-4} M) (dashed lines) in benzonitrile at 295 K for (a) $n = 3$, (b) $n = 6$, and (c) $n = 9$. The spectra were recorded with excitation at 351.1 and 363.8 nm for $n = 3$ and at 457.9 nm for $n = 6$ and 9. The dotted line in graph (c) is for the 9T/MP$-C_{60}$ mixture in benzonitrile with excitation at 600 nm, multiplied by a factor of 10 for comparison.

which increases with the polarity of the solvent. The quenching of the MP$-C_{60}(S_1)$ emission in polar solvents after excitation of the oligothiophene moiety demonstrates a significant change in the photophysical processes in comparison with the energy transfer observed in toluene. In fact, the quenching may result either from a rapid relaxation of the MP$-C_{60}(S_1)$ state or from an ultrafast process that prevents the energy transfer from *n*T-(S_1) to MP$-C_{60}(S_1)$ from occurring. To investigate whether an electron-transfer reaction is responsible for this observed fluorescence quenching, we have recorded the PIA spectra of mixtures of *n*T and MP$-C_{60}$, as well as those of the $C_{60}-n$T$-C_{60}$ triads, in both *o*-dichlorobenzene and benzonitrile.

Figure 11 shows the PIA spectra of the mixtures and triads recorded in benzonitrile solutions. Similar spectra were observed for solutions in *o*-dichlorobenzene (Figure 12). The PIA spectrum of a 2:1 mixture of MP$-C_{60}$ and 3T in benzonitrile (Figure 11a) shows the characteristic signal of MP$-C_{60}(T_1)$. Apparently, triplet energy transfer to the MP$-C_{60}(T_1)$ state also occurs for 3T in the solvents more polar than toluene (Figure 9b). In contrast, the PIA spectra of 6T and 9T mixed in a 1:2 molar ratio with MP$-C_{60}$ in benzonitrile solvents show the two characteristic and intense polaron bands of the $6T^{+\bullet}$ (at 0.84 and 1.59 eV) and $9T^{+\bullet}$ (at 0.69 and 1.45 eV) radical cations, together with a less intense transition of the MP$-C_{60}^{-\bullet}$ radical anion at 1.24 eV (Figure 11b,c).[32,33] For *o*-dichlorobenzene, the bands of $6T^{+\bullet}$ are observed at 0.82 and 1.55 eV and those of $9T^{+\bullet}$ at 0.70 and 1.45 eV, while the MP$-C_{60}^{-\bullet}$ radical anion shows a band at 1.24 eV. The PIA bands of the nT$^{+\bullet}$ radical cations in these *n*T/MP$-C_{60}$ mixtures are more intense by at least 2 orders of magnitude than the nT$^{+\bullet}$ signals that can be observed for the *n*T in the same solvents, which result from an electron-transfer reaction to the solvent. We conclude that the radical ions are formed in an *inter*molecular photoinduced electron-transfer reaction between *n*T and MP$-C_{60}$. Under the conditions of these PIA experiments, the fluorescence of 6T and 9T is not significantly quenched. This indicates that the electron transfer does not occur from the (short-lived) nT(S_1) state; rather, electron transfer takes place from the (long-lived) nT(T_1) state. It must be noted that the photoinduced electron transfer between 6T or 9T and MP$-C_{60}$ can also be achieved via selective photoexcitation of MP$-C_{60}$ at 600 nm. As an example, Figure 11c shows that identical PIA spectra are obtained for 9T/MP$-C_{60}$ mixtures, irrespective of whether excitation takes place at 458 or 600 nm. By excitation at 600 nm, the *inter*molecular photoinduced charge-transfer reaction proceeds via the MP$-C_{60}(T_1)$ state, which is reduced by neutral *n*T ($n = 6$ or 9), and again, the fluorescence of MP$-C_{60}(S_1)$ is not significantly quenched.

Figure 13 shows the changes in transmission ($-\Delta T$) as a function of the modulation frequency (ω) for the various transitions observed in the PIA spectra (Figure 11). For 3T/MP$-C_{60}$ in benzonitrile, the lifetime of the MP$-C_{60}(T_1)$ state, as determined by fitting the data to eq 1, is 380 μs. For the 6T/MP$-C_{60}$ and 9T/MP$-C_{60}$ mixtures in benzonitrile, the change in transmission ($-\Delta T$) scales with the square root of the pump-intensity dependence. This indicates that radical ions decay via a bimolecular decay mechanism. To obtain an estimate

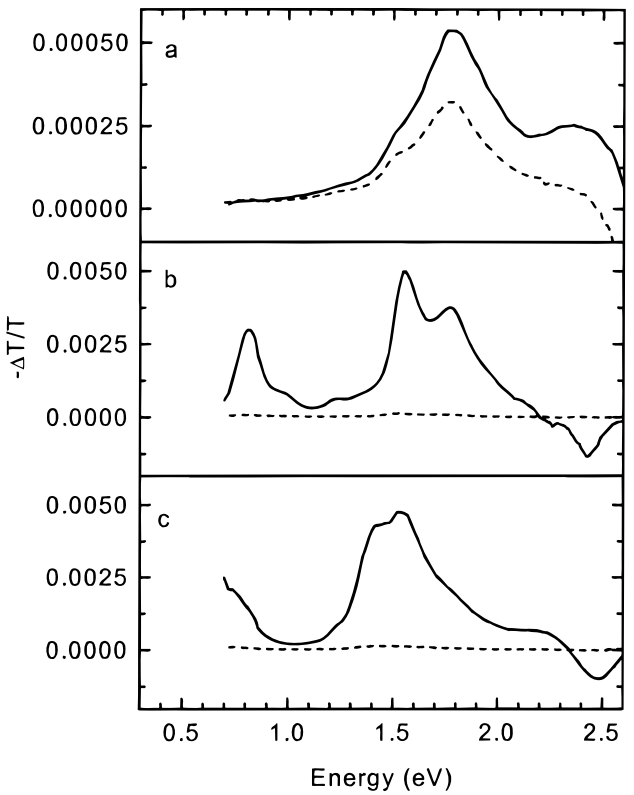

Figure 12. PIA spectra of *n*T (2.3×10^{-4} M) co-dissolved with MP−C_{60} (4.6×10^{-4} M) (solid lines) and of corresponding C_{60}−*n*T−C_{60} triads (2.3×10^{-4} M) (dashed lines) in *o*-dichlorobenzene at 295 K for (a) $n = 3$, (b) $n = 6$, and (c) $n = 9$. The spectra were recorded with excitation at 351.1 and 363.8 nm for $n = 3$ and at 457.9 nm for $n = 6$ and 9.

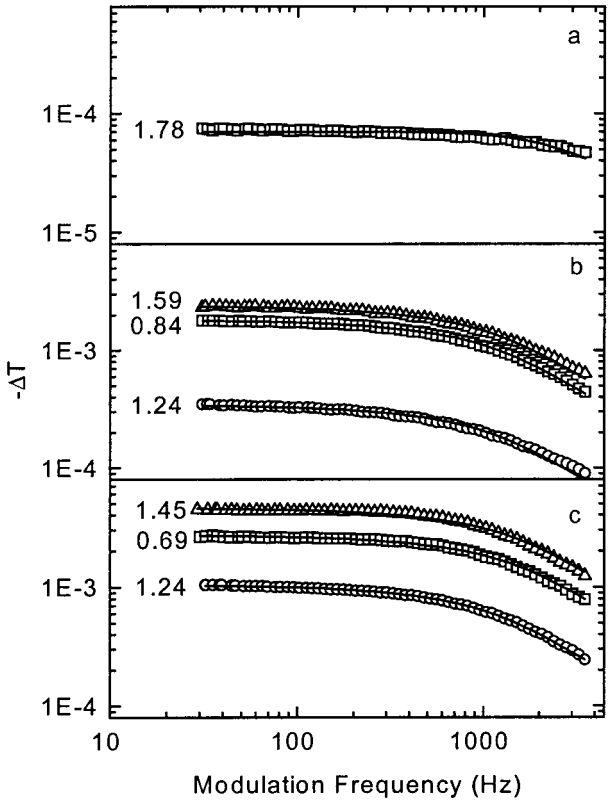

Figure 13. Modulation-frequency dependence of the PIA spectra shown in Figure 11 for the *n*T/MP−C_{60} mixtures with (a) $n = 3$, (b) $n = 6$, and (c) $n = 9$. The data were recorded at the peak positions indicated in the legends. Solid lines represent least-squares fits to the expression for monomolecular decay (a) and bimolecular decay (b and c).

of the lifetime, we fit the data shown in Figure 13b and c to the expression for bimolecular decay[27]

$$-\Delta T \propto \sqrt{Ig/\beta}\,\frac{\alpha \tanh \alpha}{\alpha + \tanh \alpha} \qquad (3)$$

where $\alpha = \pi/(\omega\tau_b)$, g is the efficiency of generation of the photoinduced species, $\tau_b = (gI\beta)^{-0.5}$ is the bimolecular lifetime under steady-state conditions, and β is the bimolecular decay constant. Equation 3 shows that the lifetime of the charged photoexcitations in the *n*T/MP−C_{60} mixtures will depend on the experimental conditions (concentration and pump intensity). Indeed, with variations in the concentration and excitation energies, different modulation frequency dependencies have been observed. Fitting the data shown in Figure 13 gives a lifetime of 1.8−1.9 ms for the $6T^{+\bullet}$ and MP−$C_{60}^{-\bullet}$ charge-separated state and a lifetime of 1.4−1.5 ms for the $9T^{+\bullet}$ and MP−$C_{60}^{-\bullet}$ combination in benzonitrile.

The PIA spectra of the C_{60}−*n*T−C_{60} triads dissolved in benzonitrile and *o*-dichlorobenzene depicted in Figures 11 and 12 are of low intensity. For C_{60}−3T−C_{60}, a weak MP−$C_{60}(T_1)$ spectrum is observed (Figure 11), while for C_{60}−6T−C_{60} and C_{60}−9T−C_{60}, the signal intensity is below 2×10^{-4}. The virtual absence of PIA bands for C_{60}−6T−C_{60} and C_{60}−9T−C_{60} in these more polar solvents is consistent with a fast forward electron-transfer reaction, resulting in a short-lived *intra*molecularly charge-separated state that decays to the ground state and is not detected with near-steady-state PIA. For most covalent donor−acceptor systems incorporating C_{60}, the lifetime of the charge-separated state is limited to the (sub)nanosecond time domain.[6−18] In general, species with lifetimes less than ~10 μs are below the detection limit ($-\Delta T/T \sim 10^{-6}$) of our PIA technique because the steady-state concentration that can be obtained is too low. At this point, it is important to note that the experiments on the *n*T/MP−C_{60} mixtures have shown that *inter*molecular electron transfer is possible for $n = 6$ and 9. Because *inter*molecular electron transfer is energetically less favorable than *intra*molecular electron transfer because of the increased distance between the opposite charges, one can conclude that *intra*molecular electron transfer is energetically allowed in cases where *inter*molecular charge transfer occurs.

Although not clearly visible from Figure 11b and c, low-intensity signals corresponding to a charged $nT^{+\bullet}$ state can be discerned for C_{60}−6T−C_{60} and C_{60}−9T−C_{60} in benzonitrile with an intensity of $-\Delta T/T$ on the order of $\sim 5 \times 10^{-6}$. For solutions in *o*-dichlorobenzene, the corresponding signals are stronger ($\sim 1 \times 10^{-4}$), but still significantly less than those of the *n*T/MP−C_{60} mixtures. Surprisingly, the modulation-frequency dependence of these low-intensity PIA signals indicates a long-lived charged state (~10 ms). These low-intensity long-lived $nT^{+\bullet}$ signals must be attributed to an *inter*molecular charge-separated state. This long-lived state can originate either from a direct electron transfer from the initially formed C_{60}−*n*T−$C_{60}(S_1)$ state to the solvent molecules or from electron or hole exchange of the transient C_{60}−$nT^{+\bullet}$−$C_{60}^{-\bullet}$ charge-separated state with a neutral triad, giving rise to separated C_{60}−$nT^{+\bullet}$−C_{60} and C_{60}−*n*T−$C_{60}^{-\bullet}$ radical ions.

Although we have not been able to obtain direct spectral confirmation of the transient charge-separated state in the triads, the PIA experiments and the quenching of the fullerene MP−$C_{60}(S_1)$ emission are strong indications that a photoinduced *intra*molecular electron-transfer reaction occurs in C_{60}−6T−

C_{60} and $C_{60}-9T-C_{60}$ in polar solvents. In the following section, we discuss the energetics of the electron-transfer process in more detail and show that our conclusions are in agreement with predictions based on the Weller equation.[34]

Energetic Considerations for Electron Transfer. Photoinduced electron transfer in solution is governed by the change in free energy for charge separation, ΔG_{cs}, given by the Weller equation, which includes terms for charge separation and solvation of the radicals ions in addition to the energies for oxidation, reduction, and excitation.[34]

$$\Delta G_{cs} = e[E_{ox}(D) - E_{red}(A)] - E_{00} - \frac{e^2}{4\pi\epsilon_0\epsilon_s R_{cc}} - \frac{e^2}{8\pi\epsilon_0}\left(\frac{1}{r^+} + \frac{1}{r^-}\right)\left(\frac{1}{\epsilon_{ref}} - \frac{1}{\epsilon_s}\right) \quad (4)$$

In this equation, $E_{ox}(D)$ and $E_{red}(A)$ are the oxidation and reduction potentials of the donor and acceptor, respectively, measured in volts vs SCE in a solvent with relative permittivity ϵ_{ref}; E_{00} is the energy of the excited state from which electron transfer occurs; R_{cc} is the center-to-center distance of the positive and negative charges in the charge separated state; r^+ and r^- are the radii of the positive and negative ions, respectively; ϵ_s is the relative permittivity of the solvent; and $-e$ and ϵ_0 are the electron charge and the vacuum permittivity, respectively.

To describe the change in free energy for photoinduced electron-transfer reactions in the $C_{60}-n$T$-C_{60}$ triads and nT/MP$-C_{60}$ mixtures using eq 4 we measured the oxidation potentials of the nT oligomers [$E_{ox}(3T) = +1.07$ V, $E_{ox}(6T) = +0.84$ V, and $E_{ox}(9T) = +0.66$ V] and the first reduction potential of MP$-C_{60}$ [$E_{red}(MP-C_{60}) = -0.67$ V] in dichloromethane ($\epsilon_{ref} = 8.93$) vs SCE. For 3T, the electrochemical oxidation is chemically irreversible, whereas the oxidation of 6T and 9T and the reduction of MP$-C_{60}$ are chemically and electrochemically reversible. The value of E_{00} was set to 1.50 eV, equal to the triplet energy of MP$-C_{60}$. Of course, a photoinduced electron-transfer reaction may originate from a higher excited state, such as nT(S_1) or MP$-C_{60}$(S_1), but the triplet level of MP$-C_{60}$ corresponds to the lowest neutral excitonic level in the triads and mixtures [assuming that the 9T(T_1) and MP$-C_{60}$(T_1) levels are energetically degenerate]. Hence, one could argue that any charge-separated state with an energy higher than $E_{00} = 1.50$ eV could eventually decay to this long-lived triplet state. The R_{cc} distances have been determined by molecular modeling of the $C_{60}-n$T$-C_{60}$ triads assuming that the positive and negative charges are localized at the centers of the oligothiophene and fullerene moieties. This leads to $R_{cc} = 10.0$ Å for $C_{60}-3T-C_{60}$, $R_{cc} = 15.4$ Å for $C_{60}-6T-C_{60}$, and $R_{cc} = 21.1$ Å for $C_{60}-9T-C_{60}$ for *intra*molecular charge transfer. For *inter*molecular charge transfer, R_{cc} was set to infinity. The value of $r^- = 5.6$ Å for C_{60} has been calculated by Verhoeven et al. from the density of C_{60}.[6i] Although we are aware that defining a single radius for one-dimensionally extended molecules such as the nT oligomers is a strong simplification of the actual situation, we estimated the values for r^+ for the oligothiophenes using a similar approach. For unsubstituted terthiophene, the density $\rho = 1.509$ g cm^{-3} is known from an X-ray crystallographic study,[35] and the radius has been determined from $r^+(3T) = (3 \times 10^{24} M/4\pi\rho N_A)^{1/3}$ to be 4.03 Å. Assuming similar densities for unsubstituted 6T and 9T, we estimate $r^+(6T) = 5.08$ Å, and $r^+(9T) = 5.80$ Å. The value for 6T corresponds well to the value of 5.02 Å that can be derived from the X-ray crystallographic data of unsubstituted sexithiophene.[36] In this approximation, we have discarded the dodecyl solubilizing side chains because the positive charge in the nT$^{+\bullet}$ radical ions will be localized in the thiophene rings. With these approximations, we come to the values listed in Table 4 for the change in free energy for *inter*- and *intra*molecular photoinduced charge transfer in the various solvents. The energies of the neutral and charge-separated states (Tables 2 and 4) are schematically shown in Figure 14.

TABLE 4: Free Energy Change for *Intra*molecular [$\Delta G_{cs}(R_{cc})$] and *Inter*molecular [($\Delta G_{cs}(\infty)$] Electron Transfer in $C_{60}-n$T$-C_{60}$ Triads and nT/MP$-C_{60}$ Mixtures in Different Solvents[a]

	solvent	$\Delta G_{cs}^{ref}(\infty)$ (eV)	$\Delta G_{cs}(\infty)$ (eV)	$\Delta G_{cs}(R_{cc})$ (eV)
3T	$PhCH_3$	0.23	1.17	0.54
	ODCB	0.23	0.19	0.04
	PhCN	0.23	0.01	−0.05
6T	$PhCH_3$	0.00	0.83	0.44
	ODCB	0.00	−0.03	−0.12
	PhCN	0.00	−0.20	−0.24
9T	$PhCH_3$	−0.16	0.61	0.33
	ODCB	−0.16	−0.29	−0.26
	PhCN	−0.16	−0.34	−0.37

[a] ΔG values calculated from eq 4 relative to the energy of the MP$-C_{60}$(T_1) state. $\Delta G_{cs}^{ref}(\infty)$ is defined as $e[E_{ox}(D) - E_{red}(A) - E(MP-C_{60}(T_1)]$.

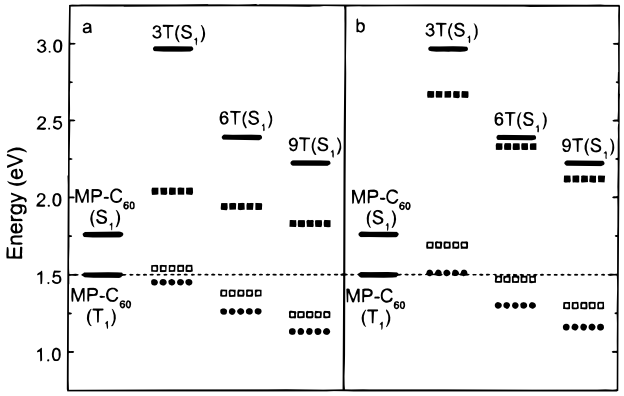

Figure 14. Excited-state energy levels. The singlet (S_1) energy levels of nT and MP$-C_{60}$ (solid bars) were determined from fluorescence data. The MP$-C_{60}$(T_1) level (solid bars and dashed line) was taken form literature phosphorescence data.[6b,6i,16a] The levels of the charge-separated states for (a) *intra*molecular charge transfer in $C_{60}-n$T$-C_{60}$ triads and (b) *inter*molecular charge transfer in nT/MP$-C_{60}$ mixtures were determined using eq 4 (see text and Table 4). Solid squares are for toluene, open squares for *o*-dichlorobenzene, and solid circles for benzonitrile solutions.

Both Table 4 and Figure 14 show that the experimentally observed photoinduced energy- and electron-transfer reactions in the $C_{60}-n$T$-C_{60}$ triads and the nT/MP$-C_{60}$ mixtures are fully accounted for by the Weller equation.

In toluene, both the MP$-C_{60}$ S_1 and T_1 states are energetically situated below a charge-separated state. Hence, *intra*- or *inter*molecular electron transfer to MP$-C_{60}$ is not expected for any of the nT oligomers in toluene, in full agreement with the fullerene fluorescence (Figure 8) and the observation of the long-lived MP$-C_{60}$(T_1) [or 9T(T_1)] state (Figure 9). It must be noted, however, that it has recently been shown that, for a geometrically constrained porphyrin−fullerene (P$-C_{60}$) dyad dissolved in toluene, the MP$-C_{60}$(T_1) state is formed via an intermediate charge-separated state.[12x] Energetically, such a process is also possible for the $C_{60}-n$T$-C_{60}$ triads if electron transfer takes place from the initially excited nT(S_1) state. The fact that fullerene fluorescence is not quenched for $C_{60}-n$T$-C_{60}$ in toluene indicates that the relaxation of such a charge-separated

state must involve the intermediacy of an MP−C_{60}(S_1) state, which was not found for the P−C_{60} dyad.[12x]

According to eq 4, both *intra*- and *inter*molecular electron transfer to the fullerene moiety become energetically favored for 6T and 9T in the more polar solvents *o*-dichlorobenzene and benzonitrile. This prediction is in full agreement with the complete quenching of the fullerene emission (Figure 10) and the observation of long-lived *inter*molecular charge-separated states with PIA spectroscopy in *n*T/MP−C_{60} mixtures (Figures 11 and 12). For C_{60}−3T−C_{60} and 3T/MP−C_{60}, a subtle evolution of the energy levels with the polarity of the solvent is apparent from Figure 14. For C_{60}−3T−C_{60}, *intra*molecular photoinduced electron transfer is energetically favored in benzonitrile in comparison with the MP−C_{60}(T_1) state ($\Delta G_{cs} = -0.05$ eV), but less likely in *o*-dichlorobenzene ($\Delta G_{cs} = +0.04$ eV) (Table 4). In accordance with this prediction, the quenching of the fullerene emission is ∼50% and ∼80%, respectively, in these solvents (Figure 10a), and in benzonitrile, only a weak MP−C_{60}(T_1) signal is observed (Figure 11a). The *inter*molecular electron transfer in 3T/MP−C_{60} is less favorable, and even in benzonitrile, a long-lived MP−C_{60}(T_1) state can be observed (Figure 11a). It must be mentioned, however, that, in this case, eq 4 predicts that the charge-separated state is only marginally higher in energy ($\Delta G_{cs} = +0.01$ eV, Table 4).

We conclude that the relative position of the various neutral and charge-separated states of the C_{60}−*n*T−C_{60} triads, as determined using the Weller equation, is in full agreement with the experimental results. Hence, from the Weller equation, we can determine a threshold permittivity for electron transfer. For *intra*molecular reactions these values are $\epsilon_s = 14.2$, 6.0, and 4.2 for $n = 3$, 6, and 9, respectively. *Inter*molecular electron transfer can take place in slightly more polar media for which $\epsilon_s = 26.5$, 8.9, and 5.7 are the corresponding thresholds. The high threshold for C_{60}−3T−C_{60} explains the observed absence of a charge-separated state in thin films of this triad.

Kinetics of Energy and Electron Transfer in Solution. Although our experiments do not have short-time resolution, it is possible to obtain a semiquantitative estimate for the kinetics of the various photophysical processes (Figure 15) on the basis of the extent of fluorescence quenching and the singlet excited-state lifetimes. The rate constants for energy transfer (k_{ET}) determined in this way (Table 3), with toluene as a solvent, indicate that *intra*molecular singlet energy transfer from *n*T-(S_1) to MP−C_{60}(S_1) occurs within about 1 ps for C_{60}−3T−C_{60} and about 100 fs for C_{60}−6T−C_{60} and C_{60}−9T−C_{60}. Because the energy of the singlet excited states is not strongly affected by the polarity of the solvent (Table 2), it is likely that similar rate constants for singlet energy transfer will apply to *o*-dichlorobenzene and benzonitrile. However, in these solvents, a photoinduced electron-transfer reaction occurs, as was shown from the quenching of the fullerene fluorescence.

In principle, the electron transfer can take place directly from the initially excited *n*T(S_1) state, but it can also occur indirectly in a two-step process via an intermediate MP−C_{60}(S_1) state (Figure 15). The fullerene emission in C_{60}−6T−C_{60} and C_{60}−9T−C_{60} in the polar solvents is about 2 orders of magnitude less than that in toluene (Figure 10, Table 3). If the electron transfer occurs after singlet energy transfer to the MP−C_{60}(S_1) state, the rate of this indirect charge separation (k_{CS}^i) can be calculated from

$$k_{CS}^{\ i} = \left[\frac{\phi(C_{60})}{\phi} - 1\right]/\tau(C_{60}) \qquad (5)$$

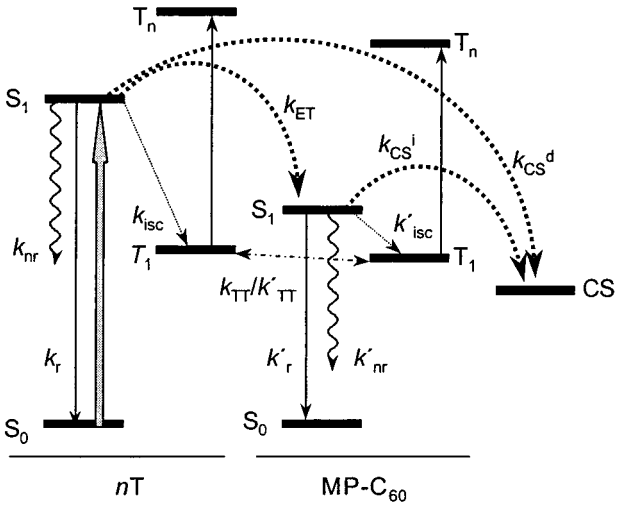

Figure 15. Schematic diagram describing energy levels of singlet (S_0, S_1), triplet (T_1, T_n), and charge-separated (CS) states of C_{60}−*n*T−C_{60} triads. The energy-transfer (k_{ET}) and indirect (k_{CS}^i) and direct (k_{CS}^d) charge-separation reactions are indicated with the curved dotted arrows. The solid arrow describes the initial excitation of the *n*T moiety. Other symbols are: k_r and k'_r for the radiative rate constants, k_{nr} and k'_{nr} for the nonradiative decay constants, k_{ics} and k'_{ics} for the intersystem crossing rate constants, and k_T and k'_{TT} for the rate constants for triplet energy transfer, each for *n*T and MP−C_{60}, respectively.

Here, $\phi(C_{60})/\phi$ is the quenching ratio of the fullerene emission and $\tau(C_{60})$ is the lifetime of the MP−C_{60}(S_1) state (1.45 ns, Table 2). The values compiled in Table 3 show that, when an indirect mechanism is operative, the electron-transfer reaction occurs in about 10−20 ps for C_{60}−6T−C_{60} and C_{60}−9T−C_{60}. If, on the other hand, electron transfer were solely due to a direct reaction from the *n*T(S_1) state (Figure 15), the decrease in fullerene emission would result from the quenching of the singlet energy transfer reaction. Under this presumption, the rate constant for a direct charge separation (k_{CS}^d) would be given by a combination of eqs 2 and 5.

$$k_{CS}^{\ d} = \left[\frac{\phi(nT)}{\phi} - 1\right]\left[\frac{\phi(C_{60})}{\phi} - 1\right]/\tau(nT) \qquad (6)$$

The values for k_{CS}^d calculated from the experimental quenching ratios (Table 3) indicate that such a transfer would be unlikely to be fast (∼1 fs). It must be noted that, in calculating these values, we assume that the rate for energy transfer is independent of the solvent polarity. In doing so, we impicitly discard the possibility that the formation of the MP−C_{60}(S_1) state in toluene involves the intermediacy of an *intra*molecularly charge-separated state. One possibility for distinguishing experimentally between the direct and indirect charge separation mechanisms would be to look for additional quenching of the *n*T luminescence in polar solvents, as this is only expected in the direct mechanism. Although some additional quenching has been observed, reliable numbers could not be obtained because of the Raman scattering of the solvents in the spectral regions of interest, which becomes significantly stronger than the residual fluorescence signal.

Further insight into the direct and indirect mechanisms can be obtained from the activation barrier for charge separation. The Marcus equation estimates the barrier for photoinduced electron transfer from the free energy change for charge separation (ΔG_{cs}) and the reorganization energy (λ).[37]

$$\Delta G_{cs}^{\ddagger} = (\Delta G_{cs} + \lambda)^2/4\lambda \qquad (7)$$

TABLE 5: Reorganization Energy (λ), Free Energy Change (ΔG_{cs}), and Barrier ($\Delta G_{cs}^{\ddagger}$) for *Intra*molecular Electron Transfer in $C_{60}-n$T$-C_{60}$ Triads in Different Solvents[a]

			*n*T(S_1)		MP$-C_{60}$(S_1)		MP$-C_{60}$(T_1)	
	solvent	λ (eV)	ΔG_{cs} (eV)	$\Delta G_{cs}^{\ddagger}$ (eV)	ΔG_{cs} (eV)	$\Delta G_{cs}^{\ddagger}$ (eV)	ΔG_{cs} (eV)	$\Delta G_{cs}^{\ddagger}$ (eV)
3T	$PhCH_3$	0.34	−0.93	0.26	0.28	0.28	0.54	0.57
	ODCB	0.81	−1.43	0.12	−0.22	0.11	0.04	0.22
	PhCN	0.93	−1.52	0.09	−0.31	0.10	−0.05	0.21
6T	$PhCH_3$	0.35	−0.45	0.007	0.18	0.20	0.44	0.46
	ODCB	0.86	−1.01	0.006	−0.38	0.07	−0.12	0.16
	PhCN	0.99	−1.13	0.005	−0.50	0.06	−0.24	0.14
9T	$PhCH_3$	0.35	−0.39	0.001	0.07	0.13	0.33	0.33
	ODCB	0.88	−0.98	0.003	−0.52	0.04	−0.26	0.11
	PhCN	1.02	−1.09	0.001	−0.63	0.04	−0.37	0.10

[a] Values calculated relative to the energies of the *n*T(S_1), MP$-C_{60}$(S_1), and MP$-C_{60}$(T_1) excited states using eqs 4, 7, and 8.

The reorganization energy is the sum of internal (λ_i) and solvent (λ_s) contributions. The solvent contribution can be calculated from the Born-Hush approach[6e,i,38]

$$\lambda_s = \frac{e^2}{4\pi\epsilon_0}\left[\frac{1}{2}\left(\frac{1}{r^+}+\frac{1}{r^-}\right)-\frac{1}{R_{cc}}\right]\left(\frac{1}{n^2}-\frac{1}{\epsilon_s}\right) \qquad (8)$$

in which n is the refractive index of the solvent. For the internal reorganization energy, we take $\lambda_i = 0.3$ eV on the basis of the value reported by Verhoeven et al. for the diethylaniline/C_{60} couple determined from the charge-transfer absorption and emission spectra. This estimate is probably an upper limit to the actual internal reorganization energy in $C_{60}-n$T$-C_{60}$, especially for the longer oligothiophenes in which a positive charge will delocalize over a large π-conjugated system, resulting in a small structural deformation and reorganization energy.[18a] The values for $\lambda = \lambda_i + \lambda_s$ obtained in this way are compiled in Table 5, together with the free energy change (ΔG_{cs}) and barrier ($\Delta G_{cs}^{\ddagger}$) for *intra*molecular electron transfer in the three $C_{60}-n$T$-C_{60}$ triads relative to the *n*T(S_1), MP$-C_{60}$(S_1), and MP$-C_{60}$(T_1) excited states. Table 5 shows a number of interesting effects. First, photoinduced electron transfer from the MP$-C_{60}$ S_1 or T_1 states is always in the "normal" Marcus region ($\lambda > -\Delta G_{cs}$). The barriers for electron transfer from the MP$-C_{60}$(S_1) state in $C_{60}-6$T$-C_{60}$ and $C_{60}-9$T$-C_{60}$ are less than ~0.1 eV in *o*-dichlorobenzene and benzonitrile. In contrast, electron transfer from the *n*T(S_1) state would occur in the Marcus "inverted" region ($\lambda < -\Delta G_{cs}$), irrespective of the solvent or the conjugation length of the *n*T donor (Table 5). The latter is a consequence of the higher energy of the singlet excited state of the *n*T oligomers in comparison with the MP$-C_{60}$ S_1 or T_1 states (Figure 14, Table 2). Because the difference between λ and $-\Delta G_{cs}$ is small for $C_{60}-6$T$-C_{60}$ and $C_{60}-9$T$-C_{60}$, the electron transfer, although formally in the inverted region, is close to the "optimal region" in these cases. As a consequence, eq 7 predicts that photoinduced electron transfer from 6T(S_1) or 9T(S_1) occurs with a very low barrier ($\Delta G_{cs}^{\ddagger} < 0.01$ eV). It is important to note that the estimates for $\Delta G_{cs}^{\ddagger}$ change only little when different values are used for λ_i: When λ_i is varied from 0.1 to 0.5 eV, $\Delta G_{cs}^{\ddagger}$ remains less than 0.05 eV for both $C_{60}-6$T$-C_{60}$ and $C_{60}-9$T$-C_{60}$ in *o*-dichlorobenzene and benzonitrile.

The energy barrier $\Delta G_{cs}^{\ddagger}$, the reorganization energy, and the electronic coupling (V) between donor and acceptor in the excited state determine the rate constant for charge separation. The expression for nonadiabatic electron-transfer processes[39]

$$k_{CS} = \left(\frac{4\pi^3}{h^2\lambda k_B T}\right)^{1/2} V^2 \exp\left(\frac{-\Delta G_{cs}^{\ddagger}}{k_B T}\right) \qquad (9)$$

allows V to be determined from the values for k_{CS}, $\Delta G_{cs}^{\ddagger}$, and λ listed in Tables 3 and 5. For the indirect mechanism, i.e., charge separation after singlet energy transfer, the values calculated for V using eq 9 and k_{CS}^{i} are in the range from 40 to 70 cm^{-1} for $C_{60}-6$T$-C_{60}$ and $C_{60}-9$T$-C_{60}$ in the two polar solvents. These values are 1 order of magnitude less than expected for a bridge consisting of three σ bonds between donor and acceptor.[6e,40] On the other hand, the values of $V = 2000-3000$ cm^{-1}, which can be calculated using k_{CS}^{d} (Table 3), assuming that only the direct mechanism is operative, are too high by 1 order of magnitude.[6e,40] Moreover, an electronic coupling of $V = 2000-3000$ cm^{-1} would certainly give rise to significant differences between the absorption spectrum of the $C_{60}-n$T$-C_{60}$ triad in comparison with the linear superposition of the spectra of *n*T and MP$-C_{60}$, which is not observed experimentally (Figure 2). On the basis of these considerations, we propose that the rate constants for electron and energy transfer are probably of the same order of magnitude. If we take the rate for direct charge separation in the polar solvents to be equal to the rate for energy transfer (i.e., 1.2×10^{13} and 9.1×10^{12} s^{-1} for $C_{60}-6$T$-C_{60}$ and $C_{60}-9$T$-C_{60}$, respectively), V is found to be between 190 and 240 cm^{-1}, and thus, it falls in the range expected for a bridge of three σ bonds.[6e,40]

In summary, we are presently not able to distinguish experimentally between direct and indirect *intra*molecular charge-separation mechanisms. Electron transfer both from the *n*T(S_1) state and from the MP$-C_{60}$(S_1) can occur with low activation barriers in polar solvents. Although the activation barriers would favor the direct mechanism, the values obtained for k_{CS}^{d} and V are improbably high. Therefore, the very fast energy transfer (~100 fs) must be at least a competitive process in the deactivation of the *n*T(S_1) states of $C_{60}-6$T$-C_{60}$ and $C_{60}-9$T$-C_{60}$. The values for k_{CS}^{i} (Table 3) serve as a lower limit to the rate of the overall charge separation process, and hence, this reaction proceeds in benzonitrile with a rate greater than or equal to 10^{11} s^{-1}. It must be stressed, however, that this value is a true lower limit because it is based on an interpretation of the experimental results in terms of the indirect process only. Higher rates for charge separation, up to 10^{13} s^{-1}, cannot be excluded from our experiments and yield values for V compatible with a dyad with three σ bonds between donor and acceptor.

Conclusions

Photoexcitation of the oligothiophene moieties of $C_{60}-n$T$-C_{60}$ triads results in a fast energy- or electron-transfer reaction to the fullerene moiety, depending on the conjugation length of the oligothiophene and the relative permittivity of the medium.

In thin solid films of these triads, energy transfer occurs for $C_{60}-3$T$-C_{60}$, whereas electron transfer takes place for $C_{60}-6$T$-C_{60}$ and $C_{60}-9$T$-C_{60}$. In solid films, the charge-separated state has a distribution of lifetimes, extending into the millisecond time domain. This long lifetime is attributed to a stabilization that results from migration of holes or electrons in the film over distances longer than the size of the molecules.

In an apolar solvent such as toluene, photoexcitation of the *n*T moiety of the $C_{60}-n$T$-C_{60}$ triads results in a singlet energy-transfer reaction to give a singlet excited MP$-C_{60}$(S_1) state, which undergoes a near-quantitative intersystem crossing to the MP$-C_{60}$(T_1) triplet state. From the strong quenching of the *n*T

fluorescence, we estimate that the energy transfer occurs within ~100 fs for $C_{60}-6T-C_{60}$ and $C_{60}-9T-C_{60}$. In more polar solvents (viz. *o*-dichlorobenzene and benzonitrile), the free energy of an *intra*molecularly charge-separated state drops below that of the $MP-C_{60}(T_1)$ triplet state (Figure 14), and an *intra*molecular photoinduced electron-transfer reaction occurs.

Similar reactions occur *inter*molecularly. In apolar solvents, triplet energy transfer takes place between *n*T and $MP-C_{60}$, whereas for *n*T/$MP-C_{60}$ mixtures in polar solvents, an *inter*molecular photoinduced electron-transfer reaction occurs for $n = 6$ and 9. It has been demonstrated that this *inter*molecularly charge-separated state can be formed from both the $nT(T_1)$ and the $MP-C_{60}(T_1)$ triplet state.

The experimentally observed *intra*- and *inter*molecular energy- and electron-transfer reactions, as a function of conjugation length and solvent permittivity, are in full agreement with the predictions based on the Weller equation, eq 4.

For the $C_{60}-n$T$-C_{60}$ triads with $n = 6$ or 9, the virtual absence of the $MP-C_{60}(S_1)$ emission provides a lower limit to the rate of the *intra*molecular photoinduced electron transfer of 10^{11} s^{-1}, assuming that charge separation occurs in an indirect mechanism after singlet energy transfer to the $MP-C_{60}(S_1)$ state (Figure 15). In this case, electron transfer is in the Marcus normal region. For a direct electron-transfer process from the $nT(S_1)$ state, the rate should be in the femtosecond regime to compete with the energy transfer. The direct electron transfer from $nT(S_1)$ is in the Marcus inverted region, and the activation barriers for charge separation are very low for $n = 6$ and 9 (Table 5). Nevertheless, the direct mechanism is not the only decay pathway because it requires improbably high values for the electronic coupling (V) between donor and acceptor in the excited state to explain the ~100-fold quenching of the fullerene fluorescence. However, when the rate for direct charge transfer is of the same order of magnitude as that for energy transfer ($\sim 10^{13}$ s^{-1}), sensible values for V (190 and 240 cm^{-1}) are found.

Although we have not been able to determine the lifetime of the *intra*molecularly charge-separated state of the $C_{60}-n$T$-C_{60}$ triads in solution, it is clearly significantly less than the lifetime of charge separation in thin films, supporting the proposition that the long lifetime in solid films of the triads is a material, rather than a molecular, property. The combination of the long lifetime of the charge-separated states of $C_{60}-6T-C_{60}$ and $C_{60}-9T-C_{60}$ in the solid state with a very fast forward electron-transfer rate is strikingly similar to the extreme asymmetry observed in conjugated polymer/(methano)fullerene blends.

Experimental Section

Absorption and Fluorescence. Optical spectra were recorded using a Perkin-Elmer Lambda 900 spectrophotometer for absorption and a Perkin-Elmer LS50B spectrophotometer equipped with a red-sensitive Hamamatsu R928−08 photomultiplier for fluorescence. The fluorescence spectra of the fullerenes were recorded with a 10-nm bandwidth in excitation and emission, and the optical density of the solutions was adjusted to 0.1 at the excitation wavelength. Fluorescence spectra were not corrected for the wavelength dependence of the sensitivity of the detection system.

Time-Resolved Fluorescence. For fluorescence lifetime measurements, a ~5 ps exciting light pulse at 300 nm was obtained by frequency doubling the output of a synchronously pumped cavity-dumped dye laser that was operated at a repetition rate of 0.48 MHz. The dye laser (operated at 600 nm) was pumped with the frequency-doubled output of an actively stabilized mode-locked Nd:YAG laser. The fluorescence light, collected in a backward-scattering geometry, was dispersed by a 0.34-m double monochromator, allowing for a spectral resolution of 1 nm. Fluorescence decay curves were recorded with the time-correlated single-photon-counting technique in reversed mode using a microchannel plate photomultiplier (Hamamatsu R3809u-51). The instrument response function was ~60 ps fwhm.

Photoinduced Absorption. Solutions for photoinduced absorption were prepared in carefully purified and rigorously deoxygenated solvents and studied in a 1-mm near-IR-grade quartz cell at room temperature. Thin films were prepared by casting from *o*-dichlorobenzene solutions on quartz and were held at 80 K using an Oxford Optistat continuous flow cryostat. PIA spectra were recorded between 0.25 and 3.5 eV by excitation with a mechanically modulated (typically 275 Hz) argon ion laser (Spectra Physics 2025) pump beam. Excitation wavelengths used in this investigation are multi-line UV (351.1−363.8 nm) or single-line 457.9 and 488.0 nm. Alternatively, the argon ion laser was used to pump a continuous-wave dye laser (Spectra Physics 375B) tuned to a wavelength of 600 nm using Rhodamine 6G. The pump power incident on the sample was typically 25 or 50 mW with a beam diameter of 2 mm. The photoinduced absorption, $-\Delta T/T \approx \Delta\alpha d$, was calculated directly from the change in transmission after correction for the fluorescence, which was recorded in a separate experiment. Photoinduced absorption spectra and fluorescence spectra were recorded with the pump beam in an almost-parallel direction to the probe beam. The lifetime of the photoexcitations was determined by recording the intensity of the PIA bands as a function of the modulation frequency (ω) in the range of 30−4000 Hz and fitting the data, after correction for the fluorescence contribution, to expressions for monomolecular or bimolecular decay.[27] Pump-intensity dependencies were obtained at 275 Hz between 10 and 100 mW and were corrected for fluorescence.

Cyclic Voltammetry. Cyclic voltammograms were recorded with 0.1 M tetrabutylammonium hexafluorophosphate (TBAH) as the supporting electrolyte using a Potentioscan Wenking POS73 potentiostat. The substrate concentration was typically 10^{-3} M. The working electrode was a platinum disc (0.2 cm^2), the counter electrode was a platinum plate (0.5 cm^2), and a saturated calomel electrode was used as the reference electrode, calibrated against the Fc/Fc^+ couple (+0.470 V vs SCE).

Synthesis and Characterization. All solvents and reagents were commercially available and used without purification, unless stated otherwise. C_{60} (99.5%) was purchased from Southern Chemical Group, LLC. Column chromatography was performed with Kieselgel Merck Type 9385 (230−400 mesh). ^1H and ^{13}C NMR spectra were recorded on a Bruker AM 400 spectrometer (400 MHz) or a Varian Unity Plus (500 MHz) instrument at 298 K. All spectra of the $C_{60}-n$T$-C_{60}$ triads were recorded in CS_2 and employed a D_2O insert as an external lock and ^1H reference ($\delta = 4.67$ ppm relative to the TMS scale) and CS_2 as an internal ^{13}C reference ($\delta = 192.3$ ppm relative to the TMS scale). Molar absorption coefficients were determined utilizing a Hewlett-Packard HP 8452 UV−Vis spectrophotometer. All HPLC analyses were performed on a Hewlett-Packard HP LC−Chemstation 3D instrument (HP 1100 Series) using an analytical Cosmosil Buckyprep column (4.6 × 250 mm). MALDI-TOF-MS spectrometry was performed on a Perseptive DE PRO Voyager MALDI-TOF spectrometer operating in negative mode, utilizing an α-cyano-4-hydroxycinnamic acid matrix.

General Procedure for Formylation of Oligothiophenes. To 3.0 mmol of DMF in 3 mL of chlorobenzene was added 3.0

mmol of $POCl_3$ at room temperature. The mixture was heated at 50 °C for 1 h, and 1.0 mmol of oligothiophene in 10 mL of chlorobenzene was added. The mixture was stirred overnight at 50 °C. After the chlorobenzene was evaporated, the mixture was refluxed in 1 M NaOH for 2 h. The dialdehyde was isolated by extraction with chloroform and purified by column chromatography.

3′-Dodecyl-[2,2′:5′,2″]terthiophene-5,5″-biscarboxaldehyde. From 0.39 g (0.9 mmol) of 3′-dodecyl-[2,2′:5′,2″]-terthiophene was obtained 0.30 g (68%) of α,ω-dialdehyde after purification by column chromatography (SiO_2, CH_2Cl_2). ^{1}H NMR ($CDCl_3$, 400 MHz): δ 9.88 (s, 1H, O═CH), 9.85 (s, 1H, O═CH), 7.71 (d, ^3J = 3.9 Hz, 1H, ThH), 7.67 (d, ^3J = 3.9 Hz, 1H, ThH), 7.24 (d, ^3J = 3.9 Hz, 1H, ThH), 7.23 (d, ^3J = 3.9 Hz, 1H, ThH), 7.19 (s, 1H, ThH), 2.78 (t, ^3J = 7.8 Hz, 2H, ThCH_2), 1.66 (dt, ^3J = 7.8 Hz, 2H, ThCH$_2$CH_2), 1.42−1.17 (m, 18H, 9CH_2), 0.86 (t, ^3J = 6.3 Hz, 3H, CH_3). ^{13}C NMR ($CDCl_3$, 100 MHz): δ 145.8 (ThC$_\alpha$), 145.0 (ThC$_\alpha$), 143.2 (ThC$_\alpha$), 135.4 (ThC$_\beta$), 131.1 (ThC$_\alpha$), 129.2 (ThC$_\beta$), 126.9 (ThC$_\beta$), 124.7 (ThC$_\beta$), 31.8 (ThCH_2), 30.1 (ThCH$_2$CH_2), 29.7−29.3 (8CH_2), 22.6 (CH_2), 14.1 (CH_3).

3′,3‴′-Didodecyl-[2,2′:5′,2″:5″,2‴:5‴,2⁗:5⁗,2⁗′]sexithiophene-5,5⁗′-biscarboxaldehyde and Regioisomers. From 102.5 mg (0.12 mmol) of β′,β‴′-didodecyl-sexithiophene was obtained 60 mg (55%) of α,ω-dialdehyde after purification by column chromatography (SiO_2, CH_2Cl_2). ^{1}H NMR ($CDCl_3$, 400 MHz): δ 9.88 (s, 1H, O═CH), 9.85 (s, 1H, O═CH), 7.70 (d, ^3J = 3.9 Hz, 1H, ThH), 7.66 (d, ^3J = 3.9 Hz, 1H, ThH), 7.22−7.02 (m, 8H, ThH), 2.79 (t, ^3J = 6.9 Hz, 2H, ThCH_2), 2.76 (t, ^3J = 6.9 Hz, 2H, ThCH_2), 1.73−1.60 (m, 4H, 2ThCH$_2$CH_2), 1.50−1.19 (m, 36H, 18CH_2), 0.88 (t, ^3J = 6.9 Hz, 3H, CH_3), 0.87 (t, ^3J = 6.9 Hz, 3H, CH_3). ^{13}C NMR ($CDCl_3$, 100 MHz): δ 146.7, 145.9, 143.0, 140.8, 137.1, 136.7, 136.3, 135.4, 134.4, 133.4, 132.3, 129.0, 128.6, 126.8, 125.7, 124.9, 124.4, 124.1, 31.9, 31.5, 30.3, 30.1, 29.9−29.3, 22.7, 14.1.

3′,3⁗′,3⁗″′-Tridodecyl-[2,2′:5′,2″:5″,2‴:5‴,2⁗:5⁗,2⁗′:5⁗′, 2⁗″′:5⁗″′,2⁗‴:5⁗‴,2⁗⁗′:5⁗⁗′,2⁗⁗″′]novithiophene-5,5⁗⁗⁗′-biscarboxaldehyde and Regioisomers. From 0.12 g (0.1 mmol) of β′,β⁗′,β⁗⁗⁗′-tridodecyl-novithiophene was obtained 78 mg (62%) of α,ω-dialdehyde after purification by column chromatography (SiO_2, CH_2Cl_2). ^{1}H NMR ($CDCl_3$, 400 MHz): δ 9.88 (s, 1H, O═CH), 9.85 (s, 1H, O═CH), 7.69 (d, ^3J = 4.2 Hz, 1H, ThH), 7.65 (d, ^3J = 4.2 Hz, 1H, ThH), 7.22−7.00 (m, 13H, ThH), 2.82−2.74 (m, 6H, 3ThCH_2), 1.75−1.55 (m, 6H, 3ThCH$_2$CH_2), 1.50−1.15 (m, 54H, 27CH$_2$), 0.92−0.80 (m, 9H, 3CH_3). ^{13}C NMR ($CDCl_3$, 100 MHz): δ 146.8, 146.0, 143.1, 140.8, 140.6, 137.5, 136.9, 136.9, 136.7, 136.4, 136.2, 135.6, 135.6, 135.2, 134.7, 134.7, 134.2, 133.4, 132.5, 129.7, 129.1, 128.5, 126.9, 126.7, 126.2, 125.7, 125.0, 124.5, 124.3, 124.1, 123.9, 31.9, 30.4, 30.2, 29.9−29.4, 22.7, 14.1.

General Procedure for Synthesis of the C$_{60}$−*n*T−C$_{60}$ Triads via Double Prato Reaction. A solution of the oligothiophene-bis-carboxaldehyde (∼1.6 mM in chlorobenzene), C_{60} (4 equiv), and sarcosine (8 equiv) was stirred and refluxed under an atmosphere of dry nitrogen for 18 h. After the mixture was cooled to room temperature, the solvent was removed in vacuo, and the remaining residue was purified by column chromatography on silicagel. Elution with carbon disulfide yielded recovered C_{60} and further elution with carbon disulfide/toluene 95/5 (v/v) afforded the pure triads.

C$_{60}$−3T−C$_{60}$. Starting from 3′-dodecyl-[2,2′:5′,2″]terthiophene-5,5″-biscarboxaldehyde (50 mg, 1.06×10^{-4} mmol), 113 mg (54%) of the pure triad was obtained. HPLC analysis (eluent, toluene; UV detection at 360 nm; flow, 1 mL/min): single peak at t_r = 9.8 min. UV−Vis [toluene, $\lambda_{max}(\epsilon)$]: 333 (83800), 432 (10030), 672 (440), 704 (710). ^{1}H NMR (CS_2, 500 MHz): δ 7.44/7.39 (2xd, J = 3.5 Hz, 2H, 2ThH), 7.15/7.12 (2xd, J = 3.5 Hz, 2H, 2ThH), 7.04 (s, 1H, ThH), 5.37/5.34 (2xs, 2H, 2NCH), 5.09 (d, J = 9.3 Hz, 2H, 2NCHH), 4.41/4.40 (2xd, J = 9.3 Hz, 2H, 2NCHH), 3.09/3.08 (2xs, 6H, 2NCH_3), 2.79 (m, 2H, ThCH_2), 1.73 (m, 2H, ThCH$_2$CH_2), 1.32−1.56 (m, 18H, 9CH_2), 1.05 (t, J = 6.8 Hz, 3H, CH_3). ^{13}C NMR (CS_2, 125 MHz): δ 155.50, 155.46, 153.44, 152.71, 152.67, 152.54, 147.09, 146.57, 146.53, 146.16, 146.14, 146.09, 146.08, 146.06, 146.04, 146.02, 145.99, 145.94, 145.93, 145.89, 145.75, 145.55, 145.52, 145.50, 145.48, 145.44, 145.24, 145.22, 145.17, 145.10, 145.08, 145.05, 145.04, 144.98, 144.96, 144.52, 144.50, 144.46, 144.17, 144.16, 142.97, 142.84, 142.54, 142.53, 142.44, 142.43, 142.09, 142.07, 142.00, 141.97, 141.94, 141.88, 141.85, 141.81, 141.77, 141.76, 141.75, 141.72, 141.65, 141.49, 141.46, 140.52, 140.14, 140.05, 140.04, 139.87, 139.84, 139.71, 139.67, 139.53, 138.34, 137.12, 136.97, 136.87, 136.53, 136.50, 135.73, 135.68, 135.46, 135.42, 135.23, 129.82, 128.48, 128.04, 126.70, 125.01, 122.78, 79.13, 79.09, 76.93, 76.84, 69.85, 68.44, 40.32, 40.29, 32.35, 30.79, 30.18, 30.12, 30.06, 29.85, 29.77, 23.37, 14.72. MALDI-TOF calcd for $C_{150}H_{42}S_3N_2$, 1968.2; found, 1967.6.

C$_{60}$−6T−C$_{60}$. Starting from 3′,3‴′-didodecyl-[2,2′:5′,2″:5″,2‴:5‴,2⁗:5⁗,2⁗′]sexithiophene-5,5⁗′-biscarboxaldehyde and regioisomers (50 mg, 5.63×10^{-5} mmol), 72 mg (54%) of the pure triad was obtained. HPLC-analysis (eluent, toluene; detection, λ = 450 nm; flow, 1 mL/min): three overlapping peaks at t_r = 7.7, 8.3, and 9.0 min. UV−Vis [toluene, $\lambda_{max}(\epsilon)$]: 326 (91070), 433 (63200), 671 (460), 704 (690). ^{1}H NMR (CS_2, 500 MHz): δ 7.45/7.40 (2xd, J = 3.9 Hz, 2H, 2ThH), 7.02−7.19 (m, 8H, 8ThH), 5.38/5.35 (2xs, 2H, 2NCH), 5.10 (2xd, 2H, 2NCHH), 4.41 (2xd, 2H, 2NCHH), 3.10/3.09 (2xs, 6H, 2NCH_3), 2.88/2.81 (2xm, 4H, 2ThCH_2), 1.82/1.74 (2xm, 4H, 2ThCH$_2$CH_2), 1.34−1.60 (m, 36H, 18CH_2), 1.44 (2xt, 6H, 2CH_3). ^{13}C NMR (CS_2, 125 MHz): δ 155.54, 155.49, 153.46, 152.74, 152.69, 152.56, 147.12, 146.60, 146.56, 143.00, 142.86, 142.56, 142.47, 142.45, 142.12, 142.10, 142.02, 142.00, 141.96, 141.90, 141.88,141.83, 141.80, 141.78, 141.74, 141.68, 141.51, 141.49. 146.17, 146.16,146.11, 146.09, 146.04, 146.01, 145.96, 145.95, 145.91, 145.77, 145.57, 145.55, 145.52, 145.45, 145.25, 145.20, 145.10, 145.08, 145.00, 144.54, 144.49, 144.19, 140.58, 140.24, 140.07, 139.90, 139.87, 139.78, 139.70, 139.56, 138.34, 137.12, 137.01, 136.91, 136.75, 136.71, 136.55, 136.52, 136.09, 135.90, 135.86, 135.76, 135.71, 135.49, 135.44, 135.22, 134.98, 129.85, 129.83, 129.78, 128.53, 128.08, 126.74, 126.62, 126.36, 125.05, 124.35, 124.30, 123.97, 123.92, 122.85, 79.17, 79.12, 76.96, 76.87, 69.88, 68.47, 40.33, 32.37, 30.80, 30.17, 30.13, 30.01, 29.85, 29.78, 23.37, 14.71. MALDI-TOF calcd for $C_{174}H_{72}S_6N_2$, 2382.9; found, 2382.1.

C$_{60}$−9T−C$_{60}$. Starting from 3′,3⁗′,3⁗⁗⁗′-tridodecyl-[2,2′:5′,2″:5″,2‴:5‴,2⁗:5⁗,2⁗′:5⁗′,2⁗″′:5⁗″′,2⁗‴:5⁗‴,2⁗⁗′:5⁗⁗′,2⁗⁗″′]-novithiophene-5,5⁗⁗⁗′-biscarboxaldehyde and regioisomers (50 mg, 3.84×10^{-5} mmol), 60 mg (56%) of the pure triad was obtained. HPLC-analysis (eluent, toluene; detection, λ = 450 nm; flow, 1 mL/min): three overlapping peaks at t_r = 6.8, 7.4, and 8.1 min. UV−Vis [toluene, $\lambda_{max}(\epsilon)$]: 331 (92280), 456 (84800), 671 (480), 704 (690). ^{1}H NMR (CS_2, 500 MHz): δ 7.45/7.41 (2xd, J = 3.9 Hz, 2H, ThH), 7.00−7.24 (m, 13H, 13ThH), 5.38/5.36 (2xs, 2H, 2NCH), 5.11/5.10 (2xd, J = 9.8 and 9.3 Hz, 2H, 2NCHH), 4.42/4.41 (2xd, J = 9.8 and 9.3 Hz, 2H, 2NCHH), 3.10/3.09 (2xs, 6H, 2NCH_3), 2.89/2.81 (2xm, 6H, 3ThCH_2), 1.83/1.75 (2xm, 6H, 3ThCH$_2$CH_2), 1.28−1.68 (m, 54H, 27CH_2), 1.05 (m, 9H, 3CH_3). ^{13}C NMR (CS_2, 125 MHz): δ 155.53, 155.48, 153.44, 152.72, 152.68, 152.55, 147.10,

147.09, 146.59, 146.55, 146.17, 146.15, 146.11, 146.10, 146.08, 146.04, 146.03, 146.00, 145.95, 145.94, 145.90, 145.76, 145.56, 145.54, 145.50, 145.49, 145.44, 145.25, 145.24, 145.18, 145.11, 145.09, 145.06, 145.04,144.99, 144.98, 144.52, 144.51, 144.47, 144.17, 142.98, 142.84, 142.55, 142.54, 142.46, 141.79, 141.77, 141.76, 141.73, 141.67, 141.50, 141.48, 140.57, 140.22, 140.14, 140.11, 140.06, 139.88, 139.85, 139.77, 139.69, 139.55, 138.33, 137.11, 136.99, 136.89, 136.76, 136.74,136.73, 136.70, 136.53, 136.50, 136.10, 136.05, 135.92, 135.88, 135.84, 135.74, 135.69, 135.47, 135.42, 135.21, 135.19, 134.96, 134.94, 129.84, 129.82, 129.77, 129.76,128.52, 128.06, 126.73, 126.61, 126.35, 125.04, 124.35, 124.29, 123.97, 123. 91, 122.83, 79.15, 79.10, 76.95, 76.86, 69.87, 68.45, 40.32, 40.29, 32.36, 32.34, 30.79, 30.76, 30.16, 30.11, 30.05, 29.99, 29.85, 29.84, 29.76, 23.37, 23.35, 14.71, 14.68. MALDI-TOF calcd for $C_{198}H_{102}S_9N_2$, 2797.5; found, 2796.8.

Acknowledgment. We thank Mr. J. L. J. van Dongen for recording the MALDI-TOF mass spectra. This work is supported by The Netherlands Organization for Energy and Environment (NOVEM) in the NOZ-PV program (146.120-008.1 and 146.120.008.3); the Dutch Ministry of Economic Affairs, the Ministry of Education, Culture and Science, and the Ministry of Housing, Spatial Planning and the Environment through the E.E.T. program (EETK97115) and the IOP Program Electro-optics (IOE95008); and by the Council for Chemical Sciences of The Netherlands Organization for Scientific Research (CW-NWO) and the Eindhoven University of Technology in the PIONIER program (98400).

References and Notes

(1) (a) Sariciftci, N. S.; Smilowitz, L.; Heeger, A. J.; Wudl, F. *Science* **1992**, *258*, 1474−1476. (b) Sariciftci, N. S.; Heeger, A. J. In *Handbook of Organic Conductive Molecules and Polymers*; Nalwa, H. S., Ed.; Wiley: New York, 1996.

(2) Yu, G.; Gao, Y.; Hummelen, J. C.; Wudl, F.; Heeger, A. J. *Science* **1995**, *270*, 1789−1791.

(3) (a) Kraabel, B.; McBranch, D.; Sariciftci, N. S.; Moses, D.; Heeger, A. J. *Phys. Rev. B* **1994**, *50*, 18543−18552. (b) Kraabel, B.; Hummelen, J. C.; Vacar, D.; Moses, D.; Sariciftci, N. S.; Heeger, A. J. *J. Chem. Phys.* **1996**, *104*, 4267−4273.

(4) (a) Smilowitz, L.; Sariciftci, N. S.; Wu, R.; Gettinger, C.; Heeger, A. J.; Wudl, F. *Phys. Rev. B* **1993**, *47*, 13835−13842. (b) Meskers, S. C. J.; van Hal, P. A.; Spiering, A. J. H.; van der Meer, A. F. G.; Hummelen, J. C.; Janssen, R. A. J. *Phys. Rev. B*, submitted.

(5) Yang, C. Y.; Heeger, A. J. *Synth. Met.* **1996**, *83*, 85−88.

(6) (a) Thomas, K. G.; Biju, V.; Guldi, D. M.; Kamat, P. V.; George, M. V. *J. Phys. Chem. B* **1999**, *103*, 8864−8869. (b) Thomas, K. G.; Biju, V.; George, M. V.; Guldi, D. M.; Kamat, P. V. *J. Phys. Chem. A* **1998**, *102*, 5341−5348. (c) Sun, Y. P.; Ma, B.; Bunker, C. E. *J. Phys. Chem. A* **1998**, *102*, 7580−7590. (d) Ma, B.; Bunker, C. E.; Guduru, R.; Zhang, X. F.; Sun, Y. P. *J. Phys. Chem. A* **1997**, *101*, 5626−5632. (e) Williams, R. M.; Koeberg, M.; Lawson, J. M.; An, Y. Z.; Rubin, Y.; Paddon-Row, M. N.; Verhoeven, J. W. *J. Org. Chem.* **1996**, *61*, 5055−5062. (f) Lawson, J. M.; Oliver, A. M.; Rotenfluh, D. F.; An, Y. Z.; Ellis, G. A.; Ranasinghe, M. G.; Khan, S. I.; Franz, A. G.; Ganapathi, P. S.; Sheppard, M. J.; Paddon-Row, M. N.; Rubin, Y. *J. Org. Chem.* **1996**, *61*, 5032−5054. (g) Nakamura, Y.; Minowa, T.; Hayashida, Y.; Tobita, S.; Shizuka, H.; Nishimura, J. *J. Chem. Soc., Faraday Trans.* **1996**, *92*, 377−382. (h) Williams, R. M.; Crielaard, W.; Hellingwerf, K. J.; Verhoeven, J. W. *Recl. Trav. Chim. Pays-Bas* **1996**, *115*, 72−76. (i) Williams, R. M.; Zwier, J. M.; Verhoeven, J. W. *J. Am. Chem. Soc.* **1995**, *117*, 4093−4099. (j) Maggini, M.; Scorrano, G.; Prato, M. *J. Am. Chem. Soc.* **1993**, *115*, 9798−9799.

(7) (a) Yamashiro, T.; Aso, Y.; Otsubo, T.; Tang, H.; Harima, Y.; Yamashita, K. *Chem. Lett.* **1999**, 443−444. (b) Knorr, S.; Grupp, A.; Mehring, M.; Grube, G.; Effenberger, F. *J. Chem. Phys.* **1999**, *110*, 3502−3508. (c) Effenberger; F.; Grube, G. *Synthesis* **1998**, 1372−1379. (d) Ferraris, J. P.; Yassar, A.; Loveday, D. C.; Hmyene, M. *Opt. Mater.* **1998**, *9*, 34−42. (e) Benincori, T.; Brenna, E.; Sannicolo, F.; Trimarco, L.; Zotti, G.; Sozzani, P. *Angew. Chem., Int. Ed. Engl.* **1996**, *35*, 648−651.

(8) Nierengarten, J. F.; Eckert, J. F.; Nicoud, J. F.; Ouali, L.; Krasnikov, V.; Hadziioannou, G. *Chem. Commun.* **1999**, 617−618.

(9) Liu, S.-G.; Shu, L.; Rivera, J.; Liu, H.; Raimundo, J.-M.; Roncali, J.; Gorgues, A.; Echegoyen, L. *J. Org. Chem.* **1999**, *64*, 4884−4886.

(10) (a) Simonsen, K. B.; Konovalov, V. V.; Konovalova, T. A.; Kawai, T.; Cava, M. P.; Kispert, L. D.; Metzger, R. M.; Becher, J. *J. Chem. Soc., Perkin Trans. 2* **1998**, 657−665. (b) Llacay, J.; Veciana, J.; Vidal-Gancedo, J.; Bourdelande, J. L.; González-Moreno, R.; Rovira, C. *J. Org. Chem.* **1998**, *63*, 5201−5210. (c) Martin, N.; Pérez, I.; Sanchez, L.; Seoane, C. *J. Org. Chem.* **1997**, *62*, 5690−5692. (d) Ravaine, S.; Delhaès, P.; Leriche, P.; Salle, M. *Synth. Met.* **1997**, *87*, 93−95. (e) Llacay, J.; Mas, M.; Molins, E.; Veciana, J.; Powell, D.; Rovira, C. *Chem. Commun.* **1997**, 659−660.

(11) Imahori, H.; Cardoso, S.; Tatman, D.; Lin, S.; Noss, L.; Seely, G. R.; Sereno, L.; Chessa de Silber, J.; Moore, T. A.; Moore, A. L.; Gust, D. *Photochem. Photobiol.* **1995**, *62*, 1009−1014.

(12) (a) Camps, X.; Dietel, E.; Hirsch, A.; Pyo, S.; Echegoyen, L.; Hackbarth, S.; Röder, B. *Chem. Eur. J.* **1999**, *5*, 2362−2373. (b) Nierengarten, J.-F.; Schall, C.; Nicoud, J.-F. *Angew. Chem.* **1998**, *110*, 2037−2040. (c) Tamaki, K.; Imahori, H.; Nishimura, Y.; Yamazaki, I.; Shimomura, A.; Okada, T.; Sakata, Y. *Chem. Lett.* **1999**, 227−228. (d) Yamada, K.; Imahori, H.; Nishimura, Y.; Yamazaki, I.; Sakata, Y. *Chem. Lett.* **1999**, 895−896. (e) Fujitsuka, M.; Ito, O.; Imahori, H.; Yamada, K.; Yamada, H.; Sakata, Y. *Chem. Lett.* **1999**, 721−722. (f) Kuciauskas, D.; Liddell, P. A.; Lin, S.; Johnson, T. E.; Weghorn, S. J.; Lindsey, J. S.; Moore, A. L.; Moore, T. A.; Gust, D. *J. Am. Chem. Soc.* **1999**, *121*, 8604−8614. (g) Jolliffe, K. A.; Langford, S. J.; Ranasinghe, M. G.; Sheppard, M. J.; Paddon-Row, M. N. *J. Org. Chem.* **1999**, *64*, 1238−1246. (h) Da Ros, T.; Prato, M.; Guldi, D.; Alessio, E.; Ruzzi, M.; Pasimeni, L. *Chem. Commun.* **1999**, 635−636. (i) Tamaki, K.; Imahori, H.; Nishimura, Y.; Yamazaki, I.; Sakata, Y. *Chem. Commun.* **1999**, 625−626. (j) Nierengarten, J. F.; Oswald, L.; Nicoud, J. F. *Chem. Commun.* **1998**, 1545−1546. (k) Higashida, S.; Imahori, H.; Kaneda, T.; Sakata, Y. *Chem. Lett.* **1998**, 605−606. (l) Liddell, P. A.; Kuciauskas, D.; Sumida, J. P.; Nash, B.; Nguyen, D.; Moore, A. L.; Moore, T. A.; Gust, D. *J. Am. Chem. Soc.* **1997**, *119*, 1400−1405. (m) Bell, T. D. M.; Smith, T. A.; Ghiggino, K. P.; Ranasinghe, M. G.; Shephard, M. J.; Paddon-Row, M. N. *Chem. Phys. Lett.* **1997**, *268*, 223−228. (n) Imahori, H.; Yamada, K.; Hasegawa, M.; Taniguchi, S.; Okada, T.; Sakata, Y. *Angew. Chem., Int. Ed. Engl.* **1997**, *36*, 2626−2629. (o) Baran, P. S.; Monaco, R. R.; Khan, A. U.; Schuster, D. I.; Wilson, S. R. *J. Am. Chem. Soc.* **1997**, *119*, 8363−8364. (p) Imahori, H.; Hagiwara, K.; Akiyama, T.; Aoki, M.; Taniguchi, S.; Okada, T.; Shirakawa, M.; Sakata, Y. *Chem. Phys. Lett.* **1996**, *263*, 545−550. (q) Kuciauskas, D.; Lin, S.; Seely, G. R.; Moore, A. L.; Moore, T. A.; Gust, D.; Drovetskaya, T.; Reed, C. A.; Boyd, P. D. W. *J. Phys. Chem.* **1996**, *100*, 15926−15932. (r) Imahori, H.; Hagiwara, K.; Aoki, M.; Akiyama, T.; Taniguchi, S.; Okada, T.; Shirakawa, M.; Sakata, Y. *J. Am. Chem. Soc.* **1996**, *118*, 11771−11782. (s) Imahori, H.; Sakata, Y. *Chem. Lett.* **1996**, 199−200. (t) Ranasinghe, M. G.; Oliver, A. M.; Rotenfluh, D. F.; Salek, A.; Paddon-Row, M. N. *Tetrahedron Lett.* **1996**, *37*, 4797−4800. (u) Imahori, H.; Hagiwara, K.; Akiyama, T.; Taniguchi, S.; Okada, T.; Sakata, Y. *Chem. Lett.* **1995**, 265−266. (v) Drovetskaya, T.; Reed, C. A.; Boyd, P. *Tetrahedron Lett.* **1995**, *36*, 7971−7974. (w) Liddell, P. A.; Sumida, J. P.; Macpherson, A. N.; Noss, L.; Seely, G. R.; Clark, K. N.; Moore, A. L.; Moore, T. A.; Gust, D. *Photochem. Photobiol.* **1994**, *60*, 537−541. (x) Schuster, D. I.; Cheng, P.; Wilson, S. R.; Prokhorenko, V.; Katterle, M.; Holzwarth, A. R.; Braslavsky, S. E.; Klihm, K.; Williams, R. M.; Luo, C. *J. Am. Chem. Soc.* **1999**, *121*, 11599−11600.

(13) (a) Nojiri, T.; Alam, M. M.; Konami, H.; Watanabe, A.; Ito, O. *J. Phys. Chem. A* **1997**, *101*, 7943−7947. (b) Dürr, K.; Fiedler, S.; Linssen, T.; Hirsch, A.; Hanack, M. *Chem. Ber. Rec.* **1997**, *130*, 1375−1378. (c) Linssen, T. G.; Dürr, K.; Hanack, M.; Hirsch, A. *J. Chem. Soc., Chem. Commun.* **1995**, 103−104.

(14) (a) Tkachenko, N. V.; Rantala, L.; Tauber, A. Y.; Helaja, J.; Hynninen, P. H.; Lemmetyinen, H. *J. Am. Chem. Soc.* **1999**, *121*, 9378−9387. (b) Helaja, J.; Tauber, A. Y.; Abel, Y.; Tkachenko, N. V.; Lemmetyinen, H.; Kilpeläinen, I.; Hynninen, P. H. *J. Chem. Soc., Perkin Trans. 1* **1999**, *121*, 2403−2408.

(15) (a) Polese, A.; Mondini, S.; Bianco, A.; Toniolo, C.; Scorrano, G.; Guldi, D. M.; Maggini, M. *J. Am. Chem. Soc.* **1999**, *121*, 3446−3452. (b) Armspach, D.; Constable, E. C.; Diederich, F.; Housecroft, C. E.; Nierengarten, J. F. *Chem. Eur. J.* **1998**, *4*, 723−733. (c) Maggini, M.; Guldi, D. M.; Mondini, S.; Scorrano, G.; Poalucci, F.; Ceroni, P.; Roffia, S. *Chem. Eur. J.* **1998**, *4*, 1992−2000. (d) Armspach, D.; Constable, E. C.; Diederich, F.; Housecroft, C. E.; Nierengarten, J. F. *Chem. Commun.* **1996**, 2009−2010. (e) Sariciftci, N. S.; Wudl, F.; Heeger, A. J.; Maggini, M.; Scorrano, C.; Prato, M.; Bourassa, J.; Ford, P. C. *Chem. Phys. Lett.* **1995**, *247*, 510−514. (f) Maggini, M.; Donò, A.; Scorrano, G.; Prato, M. *J. Chem. Soc., Chem. Commun.* **1995**, 845−846. (g) Rasinkangas, M.; Pakkanen, T. T.; Pakkanen, T. A. *J. Organomet. Chem.* **1994**, *476*, C6−C8.

(16) (a) Guldi, D. M.; Maggini, M.; Scorrano, G.; Prato, M. *J. Am. Chem. Soc.* **1997**, *119*, 974−980. (b) Maggini, M.; Karlsson, A.; Scorrano, G.; Sandonà, G.; Farnia, G.; Prato, M. *J. Chem. Soc., Chem. Commun.* **1994**, 589−590.

(17) Diederich, F.; Dietrich-Buchecker, C.; Nierengarten, J. F.; Sauvage, J. P. *J. Chem. Soc., Chem. Commun*, **1995**, 781−782.

(18) (a) Imahori, H.; Sakata, Y. *Eur. J. Org. Chem.* **1999**, 2445−2457. (b) Martín, N.; Sánchez, L.; Illescas, B.; Pérez, I. *Chem. Rev.* **1998**, *98*, 2527−2547. (c) Imahori, H.; Sakata, Y. *Adv. Mater.* **1997**, *9*, 537−546. (d) Prato, M. *J. Mater Chem.* **1997**, *7*, 1097−1109. (e) Sakata, Y.; Imahori, H.; Tsue, H.; Higahida, S.; Akiyama, T.; Yoshizawa, E.; Aoki, M.; Yamada, K.; Hagiwara, K.; Taniguchi, S.; Okada, T. *Pure Appl. Chem.* **1997**, *69*, 1951−1956.

(19) ten Hoeve, W.; Wynberg, H.; Havinga, E. E.; Meijer, E. W. *J. Am. Chem. Soc.* **1991**, *113*, 5887−5889.

(20) van Haare, J. A. E. H.; Havinga, E. E.; van Dongen, J. L. J.; Janssen, R. A. J.; Cornil, J.; Brédas, J.-L. *Chem. Eur. J.* **1998**, *4*, 1509−1522.

(21) Wintgens, V.; Valat, P.; Garnier, F. *J. Phys. Chem.* **1994**, *98*, 228−232.

(22) (a) Guldi, D. M.; Hungerbuhler, H.; Janata, E.; Asmus, K. D. *J. Phys. Chem.* **1993**, *97*, 11258−11264. (b) Arbogast, J. W.; Darmanyan, A. P.; Foote, C. S.; Rubin, Y.; Diederich, F. N.; Alvarez, M. M.; Anz, S. J.; Whetten, R. L. *J. Phys. Chem.* **1991**, *95*, 11−12.

(23) Pasimeni, L.; Maniero, A. L.; Ruzzi, M.; Prato, M.; Da Ros, T.; Barbarella, G.; Zambianchi, M. *Chem. Commun.* **1999**, 429−430.

(24) Janssen, R. A. J.; Smilowitz, L.; Sariciftci, N. S.; Moses, D. *J. Chem. Phys.* **1994**, *101*, 1787−1798.

(25) Becker, R. S.; Seixas de Melo, J.; Maçanita, A. L.; Elisei, F. *Pure Appl. Chem.* **1995**, *67*, 9−16.

(26) Grebner, D.; Helbig, M.; Rentsch, S. *J. Phys. Chem.* **1995**, *99*, 16991−16998.

(27) Dellepiane, G.; Cuniberti, C.; Comoretto, D.; Musso, G. F.; Figari, G.; Piaggi, A.; Borghesi, A. *Phys. Rev. B* **1993**, *48*, 7850−7856.

(28) (a) Rentsch, S.; Yang, J. P.; Paa, W.; Brickner, E.; Scheidt, J.; Weinkauf, R. *Phys. Chem. Chem. Phys.* **1999**, *1*, 1707−1414. (b) Seixas de Melo, J.; Silva, L. M.; Arnaut, L. G.; Becker, R. S. *J. Chem. Phys.* **1999**, *111*, 5427−5433.

(29) Janssen, R. A. J.; Sariciftci, N. S.; Heeger, A. J. *J. Chem. Phys.* **1994**, *100*, 8641−8645.

(30) (a) Botta, C.; Luzzati, S.; Tubino, R.; Bradley, D. D. C.; Friend, R. H. *Phys. Rev. B* **1993**, *48*, 14809−14817. (b) Botta, C.; Luzzati, S.; Tubino, R.; Borghesi, A. *Phys. Rev. B* **1992**, *46*, 13008−13016.

(31) (a) Zeng, Y.; Biczok, L.; Linschitz, H. *J. Phys. Chem.* **1992**, *96*, 5237−5239. (b) Sibley, S. P.; Argentine, S. M.; Francis, A. H. *Chem. Phys. Lett.* **1992**, *188*, 187−193.

(32) Janssen, R. A. J.; Moses, D.; Sariciftci, N. S. *J. Chem. Phys.* **1994**, *101*, 9519−9527.

(33) Janssen, R. A. J.; Christiaans, M. P. T.; Pakbaz, K.; Moses, D.; Hummelen, J.-C.; Sariciftci, N. S. *J. Chem. Phys.* **1995**, *102*, 2628−2635.

(34) Weller, A. *Z. Phys. Chem. Neue Folge* **1982**, *133*, 93−98.

(35) van Bolhuis, F.; Wynberg, H.; Havinga, E. E.; Meijer, E. W.; Staring, E. J. G. *Synth. Met.* **1989**, *30*, 381−389.

(36) Horowitz, G.; Bachet, B.; Yassar, A.; Lang, P.; Demanze, F.; Fave, J.-L.; Garnier, F. *Chem. Mater.* **1995**, *7*, 1337−1341.

(37) (a) Marcus, R. A. *J. Chem. Phys.* **1965**, *43*, 679−701. (b) Marcus, R. A. *Angew. Chem., Int. Ed. Engl.* **1993**, *32*, 1111−1121.

(38) (a) Oevering, H.; Paddon-Row, M. N.; Heppener, M.; Oliver, A. M.; Cotsaris, E.; Verhoeven, J. W.; Hush, N. S. *J. Am. Chem. Soc.* **1987**, *109*, 3258−3269. (b) Kroon, J.; Verhoeven, J. W.; Paddon-Row, M. N.; Oliver, A. M. *Angew. Chem., Int. Ed. Engl.* **1991**, *30*, 1358−1361

(39) Kroon, J.; Oevering, H.; Verhoeven, J. W.; Warman, J. M.; Oliver, A. M.; Paddon-Row, M. N. *J. Phys. Chem.* **1993**, *97*, 5065−5069.

(40) Oevering, H.; Verhoeven, J. W.; Paddon-Row, M. N.; Warman, J. M. *Tetrahedron* **1989**, *45*, 4751−4766.